Wave-heat coupling in one-dimensional unbounded domains: artificial boundary conditions and an optimized Schwarz method

Franz Chouly, Pauline Klein

Wave-heat coupling in one-dimensional unbounded domains: artificial boundary conditions and an optimized Schwarz method

Franz Chouly[1] and Pauline Klein[2]

[1]Université Bourgogne Franche-Comté, Institut de Mathématiques de Bourgogne, 21078 Dijon, France
[2]Université Bourgogne Franche-Comté, Laboratoire de Mathématiques de Besançon, 25030 Besançon, France

Abstract

This paper deals with the coupling between one-dimensional heat and wave equations in unbounded subdomains, as a simplified prototype of fluid-structure interaction problems. First we build artificial boundary conditions for each subproblem so as to solve it numerically in a bounded subdomain. Then we devise an optimized Schwarz-in-time (or Schwarz Waveform Relaxation) method for the numerical solving of the coupled equations, which allows possibly different solvers and different time steps for each separated problem. Particular emphasis is made on the design of optimized transmission conditions. Notably, for this setting, the optimal transmission conditions can be expressed analytically in a very simple manner. This result is illustrated by some numerical experiments.

Key words: heterogeneous domain decomposition; optimized Schwarz method; Waveform Relaxation; wave-heat coupling; fluid-structure interaction.

1 Introduction

Optimized Schwarz methods are nonoverlapping domain decomposition methods, in which transmission conditions between subdomains are formulated in order to accelerate the convergence of the global iterative process towards the solution [25]. Recent progress has been made for optimized Schwarz methods in the context of heterogeneous domain decomposition, *i.e.* where subdomains correspond to regions with different physical properties. In this case optimized transmission conditions need to be derived according to physical transmission conditions between the unknowns and their fluxes at the interfaces: see for instance [32] for elliptic partial differential equations, [14] for Stokes-Darcy coupling and [34, 35] for fluid-structure interaction.

In this work, we study the design of optimized Schwarz methods for a one-dimensional coupled problem, that involves the heat equation on one side and the wave equation on the other side. Both equations are defined in semi-infinite, unbounded domains, and appropriate conditions at the interface ensure continuity of the velocities and fluxes. This problem is among the simplest possible prototypes for fluid-structure interaction [47] and allows to face

the very first difficulties for this category of physical problems. Furthermore, we focus on the case of infinite subdomains for each problem, since it is the easiest and most fundamental one. This implies that we need to design appropriate artificial boundary conditions, at least for numerical experiments. By the way, we also prove a stability property for the coupled problem in truncated domains with artificial boundary conditions, which has not been done before, to the best of our knowledge.

The most remarkable fact is that, in this setting, optimal transmission conditions turn out to be particularly simple. Especially, one of the two conditions involves only a local, zeroth-order operator that depends solely on the wave speed c. This means that we find a Robin-type condition which implementation is straightforward. This situation is analogous to what has been found for the one dimensional wave equation with piecewise constant wave speed, and nonoverlapping optimized Schwarz methods [28]. The other condition involves a nonlocal operator, as it happens for the heat equation alone in the context of Schwarz methods [27] (see also, e.g., [37] for artificial boundary conditions).

The plan of our paper is as follows: in Section 2 we detail the coupled problem, corresponding artificial boundary conditions and provide a global stability estimate; in Section 3 we design the optimized Schwarz-in-time method for numerical solving. Section 4 presents some numerical experiments. A conclusion is drawn in Section 5.

We use the following notations: for Ω an open set of $\mathbb{R}$, $L^2(\Omega)$ denotes the Lebesgue space of square integrable functions, and $H^s(\Omega)$ ($s \in \mathbb{R}$) Sobolev spaces of real-valued functions defined on Ω, see, e.g., [1, 39]. Sobolev norms on Ω are denoted by $\|\cdot\|_{s,\Omega}$ ($s \in \mathbb{R}$), and semi-norms by $|\cdot|_{s,\Omega}$ ($s \in \mathbb{R}$). We use the notation $\mathscr{F}_t(f)$ for the Fourier transform in time of a function f defined on a space-time domain $\Omega \times \mathbb{R}$.

2 Model problem and artificial boundary conditions

We first describe in details the coupled wave-heat problem, and then provide an equivalent version using artificial boundary conditions. Then a discretization using finite elements in space and finite differences in time is provided. Corresponding energy estimates are derived.

2.1 Wave-heat coupled problem

Let us set $\widetilde{\Omega_{\rm S}} := \mathbb{R}^-$, $\widetilde{\Omega_{\rm F}} := \mathbb{R}^+$ and $\Sigma := \overline{\Omega_{\rm S}} \cap \overline{\Omega_{\rm F}} (= \{0\})$. We consider the wave-heat coupled problem in unbounded domains:

$$
\begin{aligned}
&\text{Find } \eta : \mathbb{R}^+ \times \widetilde{\Omega_{\rm S}} \to \mathbb{R} \quad \text{and} \quad u : \mathbb{R}^+ \times \widetilde{\Omega_{\rm F}} \to \mathbb{R} \text{ such that:} \\
&\begin{cases}
\partial_t^2 \eta - c^2\, \partial_x^2 \eta = f & \text{in} \quad \mathbb{R}^+ \times \widetilde{\Omega_{\rm S}}, \\
\eta(0,\cdot) = \eta_0 & \text{in} \quad \widetilde{\Omega_{\rm S}}, \\
\partial_t \eta(0,\cdot) = \dot{\eta}_0 & \text{in} \quad \widetilde{\Omega_{\rm S}},
\end{cases} \\
&\begin{cases}
\partial_t u - \kappa\, \partial_x^2 u = g & \text{in} \quad \mathbb{R}^+ \times \widetilde{\Omega_{\rm F}}, \\
\lim\limits_{|x| \to +\infty} u(t,x) = 0 & \text{for} \quad t \in \mathbb{R}^+, \\
u(0,\cdot) = u_0 & \text{in} \quad \widetilde{\Omega_{\rm F}},
\end{cases} \\
&\begin{cases}
\partial_t \eta = u & \text{on} \quad \mathbb{R}^+ \times \Sigma, \qquad (i) \\
c^2\, \partial_{\mathbf{n_S}} \eta + \kappa\, \partial_{\mathbf{n_F}} u = 0 & \text{on} \quad \mathbb{R}^+ \times \Sigma. \qquad (ii)
\end{cases}
\end{aligned}
\tag{1}
$$

The notation $\partial_{\mathbf{n_S}}$ (resp. $\partial_{\mathbf{n_F}}$) stands for the outer normal derivative to the wave domain (resp. heat domain), so that on Σ we have $\partial_{\mathbf{n_S}} = -\partial_{\mathbf{n_F}} = \partial_x$. The constant $c > 0$ represents the wave speed, and the constant $\kappa > 0$ is the diffusion constant. The source terms are f and g. The initial conditions are provided by u_0, η_0 and $\dot{\eta}_0$. Schematically, the unknown u represents the velocity of a fluid, and the unknown η represents the displacement of an elastic structure, and thus (1) can be viewed as a simplified prototype of much more complex fluid-structure interaction problems [47]. The condition (1) (i) is an essential condition on Σ, whereas the condition (1) (ii) is a natural condition on Σ. Both ensure the continuity of velocities and fluxes, as well as an energy that remains bounded in time (the global energy of the system is dissipated due to diffusion), see, e.g., [19]. Existence and uniqueness results for fluid-structure interaction problems such as the above system (1) are provided, for bounded domains, in, e.g., [41, 47] and references therein.

For practical resolution, we shall truncate the unbounded domains $\widetilde{\Omega_{\mathrm{S}}}$ and $\widetilde{\Omega_{\mathrm{F}}}$ to bounded domains, denoted by Ω_{S} and Ω_{F} respectively, still including the interface Σ. Of course, there is no reason to use, for instance, Dirichlet boundary conditions on the external boundaries, since they are not intrinsic to the problem. The matter is to derive and use transparent boundary conditions on these external boundaries, in order to solve in the truncated domain $\Omega_{\mathrm{S}} \cup \Omega_{\mathrm{F}}$ a problem strictly equivalent to the problem posed in the whole real line $\widetilde{\Omega_{\mathrm{S}}} \cup \widetilde{\Omega_{\mathrm{F}}}$.

Define $x_S > 0$ and $x_F > 0$ such that $\Omega_S := (-x_S, 0)$, $\Omega_{\mathrm{F}} := (0, x_F)$. We then define $\Gamma_{\mathrm{S}} := \{x_S\}$ and $\Gamma_F := \{-x_F\}$ the external boundaries of the wave and the heat respectively, see Figure 1. We still use the notation $\partial_{\mathbf{n_S}}$ (resp. $\partial_{\mathbf{n_F}}$) for the outer normal derivative to the wave domain (resp. heat domain) on these external boundaries.

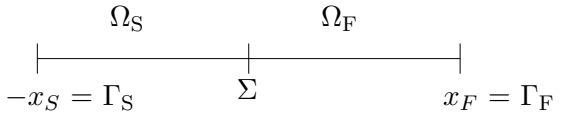

Figure 1: The truncated wave domain Ω_{S} and heat domain Ω_{F}.

In order to obtain on $\Omega_{\mathrm{S}} \cup \Omega_{\mathrm{F}}$ a problem equivalent to (1), we have to add on Γ_{S} and Γ_{F} the transparent boundary conditions. In a similar way to what has been done for instance for the linear Schrödinger equation [6, 42] these transparent boundary conditions can be explicited as follows, under the assumption that the source terms f and g are compactly supported in their respective computational domains:

$$\begin{aligned} &\partial_{\mathbf{n_S}}\eta + \frac{1}{c}\,\partial_t\eta = 0 && \text{on } \mathbb{R}^+ \times \Gamma_{\mathrm{S}}, \\ &\partial_{\mathbf{n_F}}u + \frac{1}{\sqrt{\kappa}}\,\partial_t^{\frac{1}{2}}u = 0 && \text{on } \mathbb{R}^+ \times \Gamma_{\mathrm{F}}, \end{aligned}$$

where $\partial_t^{\frac{1}{2}}$ denotes the fractional derivative in time of order one half in the sense of Riemann-Liouville (see, e.g., [43]). We also refer to [37, 48] for the derivation of transparent boundary

conditions for the heat equation. We thus transform (1) into an equivalent problem, namely:

$$
\begin{aligned}
&\text{Find } \eta : \mathbb{R}^+ \times \Omega_{\mathrm{S}} \to \mathbb{R} \quad \text{and} \quad u : \mathbb{R}^+ \times \Omega_{\mathrm{F}} \to \mathbb{R} \text{ such that:} \\
&\begin{cases}
\partial_t^2 \eta - c^2\, \partial_x^2 \eta = f & \text{in } \mathbb{R}^+ \times \Omega_{\mathrm{S}}, \\
\partial_{\mathbf{n_S}} \eta + \dfrac{1}{c}\, \partial_t \eta = 0 & \text{on } \mathbb{R}^+ \times \Gamma_{\mathrm{S}}, \\
\eta(0,\cdot) = \eta_0 & \text{in } \Omega_{\mathrm{S}}, \\
\partial_t \eta(0,\cdot) = \dot{\eta}_0 & \text{in } \Omega_{\mathrm{S}},
\end{cases} \\
&\begin{cases}
\partial_t u - \kappa\, \partial_x^2 u = g & \text{in } \mathbb{R}^+ \times \Omega_{\mathrm{F}}, \\
\partial_{\mathbf{n_F}} u + \dfrac{1}{\sqrt{\kappa}}\, \partial_t^{\frac{1}{2}} u = 0 & \text{on } \mathbb{R}^+ \times \Gamma_{\mathrm{F}}, \\
u(0,\cdot) = u_0 & \text{in } \Omega_{\mathrm{F}},
\end{cases} \\
&\begin{cases}
\partial_t \eta = u & \text{on } \mathbb{R}^+ \times \Sigma, \\
c^2 \partial_{\mathbf{n_S}} \eta + \kappa\, \partial_{\mathbf{n_F}} u = 0 & \text{on } \mathbb{R}^+ \times \Sigma.
\end{cases}
\end{aligned}
\tag{2}
$$

We now provide a weak formulation of the above problem, which will later on be discretized by finite elements in space and finite differences in time. For comparison purposes, we will derive a monolithic scheme, where the coupling conditions on the interface Σ are treated in an implicit manner at each time step, see, e.g., [18, 20]. This scheme will serve as a reference solution. We use a global space of wave and heat functions. The essential condition on Σ is then directly included into this space.

For E a subset of the boundary $\partial\Omega$, we use the classical notation for the spaces of vanishing trace on E:

$$H^1_E(\Omega) := \left\{ \varphi \in H^1(\Omega) \ ; \ \varphi|_E = 0 \right\}.$$

Let us define $V_{\mathrm{S}} \coloneqq H^1(\Omega_{\mathrm{S}})$ and $V_{\mathrm{F}} \coloneqq H^1(\Omega_{\mathrm{F}})$. From (2), we perform an integration by parts and replace the boundary terms on Γ_{S} and on Γ_{F} using the artificial boundary conditions. Introducing the global space which contains the essential condition on Σ:

$$V_{\mathrm{SF}} \coloneqq \{ (\xi, v) \in V_{\mathrm{S}} \times V_{\mathrm{F}} \ ; \ \xi|_\Sigma = v|_\Sigma \},$$

we obtain the following weak formulation:

For $t > 0$, find $\eta(t) \in V_{\mathrm{S}}$ and $u(t) \in V_{\mathrm{F}}$ satisfying $\partial_t \eta(t)|_\Sigma = u(t)|_\Sigma$, such that:

$$
\begin{cases}
\dfrac{d^2}{dt^2} \displaystyle\int_{\Omega_{\mathrm{S}}} \eta(t)\xi + \frac{d}{dt} \int_{\Omega_{\mathrm{F}}} u(t) v + \int_{\Omega_{\mathrm{S}}} c^2\, \partial_x \eta(t) \partial_x \xi + \int_{\Omega_{\mathrm{F}}} \kappa\, \partial_x u(t) \partial_x v \\
\qquad\qquad + \displaystyle\int_{\Gamma_{\mathrm{S}}} c\, \partial_t \eta(t) \xi + \int_{\Gamma_{\mathrm{F}}} \sqrt{\kappa}\, \partial_t^{\frac{1}{2}} u(t) v \\
\qquad\qquad\qquad = \displaystyle\int_{\Omega_{\mathrm{S}}} f(t)\xi + \int_{\Omega_{\mathrm{F}}} g(t) v, \qquad \forall (\xi, v) \in V_{\mathrm{SF}}.
\end{cases}
\tag{3}
$$

2.2 Energy estimate

The global (kinetic and potential elastic) energy associated to Problem (3) is defined as

$$\mathcal{E}(t) := \frac{1}{2} \left(\|\dot{\eta}(t)\|^2_{\Omega_{\mathrm{S}}} + c^2 \|\partial_x \eta(t)\|^2_{\Omega_{\mathrm{S}}} + \|u(t)\|^2_{\Omega_{\mathrm{F}}} \right), \qquad t \in \mathbb{R}^+. \tag{4}$$

Its discrete counterpart will be defined in (13) and depicted in the numerical section.

Before stating the main result of this section, we give a useful lemma (that is stated in, e.g., [2, 7, 36], with a lower regularity assumption).

Lemma 2.1. *Let $T > 0$ and $\varphi \in H^{\frac{1}{2}}(0,T)$ a function extended by zero outside $(0,T)$. We denote by $S^{\frac{\pi}{4}}$ the half-cone of the complex plane characterized by an argument comprised between $-\frac{\pi}{4}$ and $+\frac{\pi}{4}$:*

$$S^{\frac{\pi}{4}} := \left\{ z \in \mathbb{C}\,;\, \arg(z) \in \left[-\frac{\pi}{4}, +\frac{\pi}{4} \right] \right\}. \tag{5}$$

We have:

$$\int_0^T \overline{\varphi(t)}\, \partial_t^{\frac{1}{2}} \varphi(t)\, \mathrm{d}t \;\; \in S^{\frac{\pi}{4}}. \tag{6}$$

Moreover, if φ is a real-valued function, then we have:

$$\int_0^T \varphi(t)\, \partial_t^{\frac{1}{2}} \varphi(t)\, \mathrm{d}t \geqslant 0. \tag{7}$$

Proof. All along the paper, we adopt the following convention: for a complex number z, $\sqrt{z}$ is the principal determination of the square-root with branch-cut along the negative real axis. We still denote by $\varphi = \mathcal{P}\varphi$ the function φ extended by zero outside $(0,T)$. We apply the Plancherel identity in $L^2(\mathbb{R})$ for the Fourier transform in time, and use the fact that the Fourier symbol of the $\partial_t^{\frac{1}{2}}$ operator is $\sqrt{i\tau}$ (that is $\mathscr{F}_t\left(\partial_t^{\frac{1}{2}} f\right)(\tau) = \sqrt{i\tau}\, \mathscr{F}_t(f)(\tau)$). We then have:

$$\begin{aligned}
\int_0^T \overline{\varphi(t)}\, \partial_t^{\frac{1}{2}} \varphi(t)\, \mathrm{d}t &= \int_{\mathbb{R}} \overline{\varphi(t)}\, \partial_t^{\frac{1}{2}} \varphi(t)\, \mathrm{d}t \\
&= \int_{\mathbb{R}} \overline{\mathscr{F}_t(\varphi)(\tau)}\, \mathscr{F}_t\left(\partial_t^{\frac{1}{2}} \varphi\right)(\tau)\, \mathrm{d}\tau \\
&= \int_{\mathbb{R}} \overline{\mathscr{F}_t(\varphi)(\tau)}\, \sqrt{i\tau}\, \mathscr{F}_t(\varphi)(\tau)\, \mathrm{d}\tau \\
&= \int_{\mathbb{R}} |\mathscr{F}_t(\varphi)(\tau)|^2 \sqrt{i\tau}\, \mathrm{d}\tau \\
&= \int_{\mathbb{R}^-} |\mathscr{F}_t(\varphi)(\tau)|^2\, e^{-i\frac{\pi}{4}} \sqrt{-\tau}\, \mathrm{d}\tau + \int_{\mathbb{R}^+} |\mathscr{F}_t(\varphi)(\tau)|^2\, e^{i\frac{\pi}{4}} \sqrt{\tau}\, \mathrm{d}\tau \\
&= e^{-i\frac{\pi}{4}} \underbrace{\int_{\mathbb{R}^-} |\mathscr{F}_t(\varphi)(\tau)|^2 \sqrt{-\tau}\, \mathrm{d}\tau}_{\in \mathbb{R}^+} + e^{i\frac{\pi}{4}} \underbrace{\int_{\mathbb{R}^+} |\mathscr{F}_t(\varphi)(\tau)|^2 \sqrt{\tau}\, \mathrm{d}\tau}_{\in \mathbb{R}^+}.
\end{aligned}$$

The original integral is then the sum of an element of the half-line $e^{-i\frac{\pi}{4}}\mathbb{R}^+$ and of an element of the half-line $e^{i\frac{\pi}{4}}\mathbb{R}^+$. It lies then in the half-cone $S^{\frac{\pi}{4}}$. Notably, the integral is of positive real part, and if the function φ is real-valued, then the integral is real too, and positive. □

We state below the main result of this section, which is an energy stability estimate for the continuous wave-heat problem (3), in truncated domains with artificial boundary conditions. It ensures that the energy remains bounded in time for a closed system, and that the solution (η, u) to Problem (3) is unique.

Proposition 2.2. *Let us consider η and u the solutions to Problem (3) with source terms f and g identically equal to zero. Let $T > 0$ and assume that $u|_{\Gamma_F} \in H^{\frac{1}{2}}(0,T)$. Then the following inequality holds:*

$$\mathcal{E}(T) + \kappa \int_0^T \|\partial_x u(t)\|^2_{\Omega_F} \, \mathrm{d}t \leqslant \mathcal{E}(0). \tag{8}$$

Proof. We follow standard arguments already used for fluid-structure interaction systems, see, e.g., [20, Proposition 9.1], the main difference being the treatment of artificial conditions on the external boundaries. First we set test functions $\xi = \partial_t \eta(t)$, which belongs to $V_S = H^1(\Omega_S)$, and $v = u(t)$, which belongs to $V_F = H^1(\Omega_F)$. Furthermore, we have $\xi|_\Sigma = \partial_t \eta(t)|_\Sigma = u(t)|_\Sigma = v|_\Sigma$, so ξ and v coincide on Σ, and thus $(\xi, v) \in V_{SF}$. Problem (3), with source terms f and g equal to zero and with the above choice of test functions, reads:

$$\begin{aligned}\int_{\Omega_S} \frac{\partial}{\partial t}\left(\frac{\partial \eta(t)}{\partial t}\right)\frac{\partial \eta(t)}{\partial t} + \int_{\Omega_F} \frac{\partial u(t)}{\partial t}\, u(t) + \int_{\Omega_S} c^2\, \partial_x \eta(t) \partial_x \left(\partial_t \eta(t)\right) \\ + \int_{\Omega_F} \kappa\, \partial_x u(t) \partial_x u(t) + \int_{\Gamma_S} c\, \partial_t \eta(t) \partial_t \eta(t) + \int_{\Gamma_F} \sqrt{\kappa}\, u(t) \partial_t^{\frac{1}{2}} u(t) = 0\end{aligned}$$

which is equivalent to

$$\begin{aligned}\int_{\Omega_S} \frac{\partial}{\partial t}\left(\frac{1}{2}\left(\frac{\partial \eta(t)}{\partial t}\right)^2\right) + \int_{\Omega_F} \frac{\partial}{\partial t}\left(\frac{1}{2}\left(u(t)\right)^2\right) + \int_{\Omega_S} c^2 \frac{\partial}{\partial t}\left(\frac{1}{2}\left(\partial_x \eta(t)\right)^2\right) \\ + \int_{\Omega_F} \kappa\, \left(\partial_x u(t)\right)^2 + \int_{\Gamma_S} c\, \left(\partial_t \eta(t)\right)^2 + \int_{\Gamma_F} \sqrt{\kappa}\, u(t) \partial_t^{\frac{1}{2}} u(t) = 0.\end{aligned}$$

We re-write the above equality as

$$\begin{aligned}\frac{1}{2}\frac{d}{dt}\left(\left\|\frac{\partial \eta(t)}{\partial t}\right\|^2_{\Omega_S} + \|u(t)\|^2_{\Omega_F} + c^2 \|\partial_x \eta(t)\|^2_{\Omega_S}\right) + \kappa \|\partial_x u(t)\|^2_{\Omega_F} \\ = -\int_{\Gamma_S} c\, \left(\partial_t \eta(t)\right)^2 - \int_{\Gamma_F} \sqrt{\kappa}\, u(t) \partial_t^{\frac{1}{2}} u(t).\end{aligned}$$

Integrating in time, we obtain:

$$\begin{aligned}\frac{1}{2}\left(\left\|\frac{\partial \eta}{\partial t}(T)\right\|^2_{\Omega_S} + \|u(T)\|^2_{\Omega_F} + c^2 \|\partial_x \eta(T)\|^2_{\Omega_S}\right) + \kappa \int_0^T \|\partial_x u(t)\|^2_{\Omega_F} \, \mathrm{d}t \\ = -\int_0^T \int_{\Gamma_S} c\, \left(\partial_t \eta(t)\right)^2 \, \mathrm{d}t - \int_{\Gamma_F} \sqrt{\kappa} \int_0^T u(t) \partial_t^{\frac{1}{2}} u(t) \, \mathrm{d}t \\ + \frac{1}{2}\left(\|\dot{\eta}_0\|^2_{\Omega_S} + \|u_0\|^2_{\Omega_F} + c^2 \|\partial_x \eta_0\|^2_{\Omega_S}\right).\end{aligned}$$

There remains to show that the first two integrals of the right-hand side are positive. It is obvious for the first one. It is also the case for the second one, due to the properties of the $\partial_t^{\frac{1}{2}}$ operator, as stated in Lemma 2.1. We apply it to the real-valued function $u(t)|_{\Gamma_F}$, which yields:

$$\int_0^T u(t) \partial_t^{\frac{1}{2}} u(t) \, \mathrm{d}t \geqslant 0,$$

hence the stability estimate (8). □

Remark 2.1. Remark in the above result the dissipative role of both artificial boundary conditions, which are as well absorbing boundary conditions.

2.3 Space semi-discretization

We introduce for each subdomain the finite element spaces associated with $V_{\mathrm{S}} = H^1(\Omega_{\mathrm{S}})$ and $V_{\mathrm{F}} = H^1(\Omega_{\mathrm{F}})$, and with element sizes denoted by h_{S} and h_{F} respectively (h_{S} and h_{F} may have different values). We denote by $V_{\mathrm{S}}^{h_{\mathrm{S}}} \subset H^1(\Omega_{\mathrm{S}})$ and $V_{\mathrm{F}}^{h_{\mathrm{F}}} \subset H^1(\Omega_{\mathrm{F}})$ the corresponding finite element spaces based on continuous piecewise polynomial Lagrange elements of order one, and by $(\varphi_i^S)_{1\leqslant i\leqslant N}$ (resp. $(\varphi_j^F)_{1\leqslant j\leqslant M}$) the basis of hat functions associated to $V_{\mathrm{S}}^{h_{\mathrm{S}}}$ (resp. $V_{\mathrm{F}}^{h_{\mathrm{F}}}$). Thus

$$V_{\mathrm{S}}^{h_{\mathrm{S}}} \coloneqq \langle \varphi_1^S, \dots, \varphi_N^S \rangle, \qquad\qquad V_{\mathrm{F}}^{h_{\mathrm{F}}} \coloneqq \langle \varphi_1^F, \dots, \varphi_M^F \rangle.$$

Let us take test functions $\xi_{h_{\mathrm{S}}}$ and $v_{h_{\mathrm{F}}}$ belonging to the spaces $V_{\mathrm{S}}^{h_{\mathrm{S}}}$ and $V_{\mathrm{F}}^{h_{\mathrm{F}}}$ respectively. We then define the conforming space V_{SF}^h as follows:

$$V_{\mathrm{SF}}^h \coloneqq \left\{ (\xi_{h_{\mathrm{S}}}, v_{h_{\mathrm{F}}}) \in V_{\mathrm{S}}^{h_{\mathrm{S}}} \times V_{\mathrm{F}}^{h_{\mathrm{F}}} \ ; \ \xi_{h_{\mathrm{S}}}|_\Sigma = v_{h_{\mathrm{F}}}|_\Sigma \text{ on } \Sigma \right\} (\subset V_{\mathrm{SF}}).$$

For the sake of conciseness of notations, we will simply write h in the sequel instead of h_{S} and h_{F}. Yet, we keep in mind that this parameter may be given different values on the two subdomains.

The semi-discretization in space of Problem (3) is:

$$\begin{cases} \text{For } t > 0, \ \text{find } \eta_h(t) \in V_{\mathrm{S}}^{h_{\mathrm{S}}} \text{ and } u_h(t) \in V_{\mathrm{F}}^{h_{\mathrm{F}}}, \text{ such that:} \\ \dfrac{d^2}{dt^2} \displaystyle\int_{\Omega_{\mathrm{S}}} \eta_h(t)\xi_h + \frac{d}{dt} \int_{\Omega_{\mathrm{F}}} u_h(t) v_h + \int_{\Omega_{\mathrm{S}}} c^2 \, \partial_x \eta_h(t) \partial_x \xi_h + \int_{\Omega_{\mathrm{F}}} \kappa \, \partial_x u_h(t) \partial_x v_h \\ \qquad\qquad + \displaystyle\int_{\Gamma_{\mathrm{S}}} c \, \partial_t \eta_h(t) \xi_h + \int_{\Gamma_{\mathrm{F}}} \sqrt{\kappa} \, \partial_t^{\frac{1}{2}} u_h(t) v_h \\ \qquad\qquad = \displaystyle\int_{\Omega_{\mathrm{S}}} f(t)\xi_h + \int_{\Omega_{\mathrm{F}}} g(t) v_h, \qquad \forall (\xi_h, v_h) \in V_{\mathrm{SF}}^h, \\ \partial_t \eta_h(t)|_\Sigma = u_h(t)|_\Sigma. \end{cases} \tag{9}$$

Remark 2.2. A stability estimate analogous to the one stated in Proposition 2.2 can be derived following exactly the same path, so there holds:

$$\mathcal{E}_h(T) + \kappa \int_0^T \|\partial_x u_h(t)\|_{\Omega_{\mathrm{F}}}^2 \, \mathrm{d}t \leqslant \mathcal{E}_h(0),$$

where $\mathcal{E}_h$ is the semi-discrete counterpart of $\mathcal{E}$, defined identically by substituting η_h and u_h to η and u, respectively.

2.4 Fully discrete problem and monolithic scheme

We now propose to discretize in time Problem (9). For the sake of simplicity, we use the Crank-Nicolson scheme for the wave (Newmark scheme with parameters $(\beta, \gamma) = (\frac{1}{4}, \frac{1}{2})$), and the backward Euler scheme for the heat, which is a common choice for fluid-structure

interaction [18, 20]. We denote by $\delta t > 0$ the time step and use the classical notation $x^{n+\frac{1}{2}} := \frac{1}{2}(x^n + x^{n+1})$.

The discretization of the essential condition on Σ writes:

$$\frac{1}{\delta t}(\eta_h^{n+1} - \eta_h^n)|_\Sigma = u_h^{n+1}|_\Sigma. \tag{10}$$

The semi-discretized scheme (9) becomes:

Find $\eta_h^{n+1} \in V_{\mathrm{S}}^{h_{\mathrm{S}}}$, $\dot{\eta}_h^{n+1} \in V_{\mathrm{S}}^{h_{\mathrm{S}}}$ and $u_h^{n+1} \in V_{\mathrm{F}}^{h_{\mathrm{F}}}$ such that:

$$\begin{cases} \displaystyle\int_{\Omega_{\mathrm{S}}} \frac{1}{\delta t}(\dot{\eta}_h^{n+1} - \dot{\eta}_h^n)\xi_h + \int_{\Omega_{\mathrm{F}}} \frac{1}{\delta t}(u_h^{n+1} - u_h^n)v_h \\ \qquad\qquad + \displaystyle\int_{\Omega_{\mathrm{S}}} c^2\, \partial_x \eta_h^{n+\frac{1}{2}} \partial_x \xi_h + \int_{\Omega_{\mathrm{F}}} \kappa\, \partial_x u_h^{n+1} \partial_x v_h \\ \qquad\qquad + \displaystyle\int_{\Gamma_{\mathrm{S}}} \frac{c}{\delta t}(\eta_h^{n+1} - \eta_h^n)\xi_h + \int_{\Gamma_{\mathrm{F}}} \sqrt{\kappa} \left[\partial_t^{\frac{1}{2}} u_h\right]^{n+1} v_h \\ \qquad\qquad = \displaystyle\int_{\Omega_{\mathrm{S}}} f^{n+\frac{1}{2}} \xi_h + \int_{\Omega_{\mathrm{F}}} g^{n+1} v_h, \qquad\qquad \forall (\xi_h, v_h) \in V_{\mathrm{SF}}^h, \\ \displaystyle\frac{1}{\delta t}(\eta_h^{n+1} - \eta_h^n) = u_h^{n+1}, \qquad \text{on } \Sigma, \\ \displaystyle\frac{1}{\delta t}(\eta_h^{n+1} - \eta_h^n) = \dot{\eta}_h^{n+\frac{1}{2}}, \qquad \text{in } \Omega_{\mathrm{S}}. \end{cases}$$

In the above equation, the notation $\left[\partial_t^{\frac{1}{2}} u_h\right]^{n+1}$ indicates the discretization at time t^{n+1} of the term $\partial_t^{\frac{1}{2}} u_h(t)$. For instance, to be consistent with the backward Euler scheme, this discretization of the $\partial_t^{\frac{1}{2}}$ operator can be given following [40]:

$$\partial_t^{\frac{1}{2}} f^n = \frac{1}{\sqrt{\delta t}} \sum_{k=0}^{n} \beta_{n-k} f^k,$$

where the coefficients (β_k) are defined as follows:

$$\begin{cases} \beta_0 = 1 \\ \beta_k = \dfrac{(-1)^k}{k!} \displaystyle\prod_{i=0}^{k-1} \left(\frac{1}{2} - i\right), \quad \text{for } k \geqslant 1. \end{cases} \tag{11}$$

We thus obtain

$$\left[\partial_t^{\frac{1}{2}} u_h\right]^{n+1} = \frac{1}{\sqrt{\delta t}} \sum_{k=0}^{n+1} \beta_{n+1-k} u_h^k = \frac{1}{\sqrt{\delta t}}\, u_h^{n+1} + \frac{1}{\sqrt{\delta t}} \sum_{k=0}^{n} \beta_{n+1-k} u_h^k.$$

Thereby, the fully discretized problem writes:

$$
\begin{aligned}
&\text{Find } \eta_h^{n+1} \in V_{\mathrm{S}}^{h_{\mathrm{S}}},\ \dot\eta_h^{n+1} \in V_{\mathrm{S}}^{h_{\mathrm{S}}} \text{ and } u_h^{n+1} \in V_{\mathrm{F}}^{h_{\mathrm{F}}} \text{ such that:}\\
&\begin{cases}
\displaystyle\int_{\Omega_{\mathrm{S}}} \frac{1}{\delta t}(\dot\eta_h^{n+1} - \dot\eta_h^{n})\xi_h + \int_{\Omega_{\mathrm{F}}} \frac{1}{\delta t}(u_h^{n+1} - u_h^{n})v_h \\
\displaystyle + \int_{\Omega_{\mathrm{S}}} c^2\, \partial_x \eta_h^{n+\frac12} \partial_x \xi_h + \int_{\Omega_{\mathrm{F}}} \kappa\, \partial_x u_h^{n+1} \partial_x v_h \\
\displaystyle + \int_{\Gamma_{\mathrm{S}}} \frac{c}{\delta t}(\eta_h^{n+1} - \eta_h^{n})\xi_h + \int_{\Gamma_{\mathrm{F}}} \sqrt{\frac{\kappa}{\delta t}} \left(\sum_{k=0}^{n+1} \beta_{n+1-k}\, u_h^k \right) v_h, \\
\displaystyle = \int_{\Omega_{\mathrm{S}}} f^{n+\frac12}\xi_h + \int_{\Omega_{\mathrm{F}}} g^{n+1} v_h, \qquad \forall (\xi_h, v_h) \in V_{\mathrm{SF}}^h, \\
\displaystyle \frac{1}{\delta t}(\eta_h^{n+1} - \eta_h^{n}) = u_h^{n+1}, \qquad \text{on } \Sigma, \\
\displaystyle \frac{1}{\delta t}(\eta_h^{n+1} - \eta_h^{n}) = \dot\eta_h^{n+\frac12}, \qquad \text{in } \Omega_{\mathrm{S}}.
\end{cases}
\end{aligned}
\tag{12}
$$

2.5 Energy estimate for the fully discretized problem

The energy associated to the fully discrete problem (12), at time $t^n := n\delta t$, is defined as:

$$
\mathcal{E}_h^n := \frac12 \left(\|\dot\eta_h^n\|_{\Omega_{\mathrm{S}}}^2 + c^2 \|\partial_x \eta_h^n\|_{\Omega_{\mathrm{S}}}^2 + \|u_h^n\|_{\Omega_{\mathrm{F}}}^2 \right), \qquad n \in \mathbb{N}. \tag{13}
$$

First we give some useful properties of the $\mathcal{Z}$-transform, and then a result similar to Lemma 2.1. For a sequence $f = (f_n)$ of real or complex numbers, we define its $\mathcal{Z}$-transform, denoted by $\widehat{f}$ or $\mathcal{Z}(f_n)$, by

$$
\widehat{f}(z) \coloneqq \mathcal{Z}(f_n)(z) \coloneqq \sum_{n=0}^{+\infty} f_n z^{-n}, \quad \text{for } |z| > R_{\widehat{f}}, \tag{14}
$$

where $R_{\widehat{f}}$ is defined by

$$
R_{\widehat{f}} \coloneqq \inf \left\{ R > 0 \ ; \ \sum_{n=0}^{+\infty} f_n R^{-n} < +\infty \right\}.
$$

As a consequence of this definition, we have some useful properties:

(a) $\mathcal{Z}(f_{n+1})(z) = z\widehat{f}(z) - z f(0)$,

(b) $\mathcal{Z}(f_{n+1} \pm f_n)(z) = (z \pm 1)\widehat{f}(z) - z f(0)$,

(c) $\mathcal{Z}(f_n \star g_n)(z) = \widehat{f}(z)\,\widehat{g}(z), \quad \text{for } |z| > \max\left(R_{\widehat{f}}, R_{\widehat{g}}\right)$,

where $f_n \star g_n$ denotes the discrete convolution between f and g. We also have a Plancherel theorem for the $\mathcal{Z}$-transform (see, e.g., [15]).

Lemma 2.3. *Let $(f_p)_{p\in\mathbb{N}}$ and $(g_p)_{p\in\mathbb{N}}$ be two sequences. If $R_{\widehat{f}} R_{\widehat{g}} < 1$, then $\mathcal{Z}(\overline{f_p}\, g_p)$ is defined for all $|z| > R_{\widehat{f}} R_{\widehat{g}}$, and we have*

$$
\sum_{p=0}^{+\infty} \overline{f_p}\, g_p = \mathcal{Z}\left(\overline{f_p}\, g_p\right)(z=1) = \frac{1}{2\pi} \int_0^{2\pi} \overline{\widehat{f}(re^{i\theta})}\, \widehat{g}\left(\frac{e^{i\theta}}{r}\right) \mathrm{d}\theta, \tag{15}
$$

where the integration path is a circle of radius r such that $R_{\widehat{f}} < r < 1/R_{\widehat{g}}$. Furthermore, if the two radii of convergence satisfy $R_{\widehat{f}} < 1$ and $R_{\widehat{g}} < 1$, then we can choose $r = 1$ in (15).

We now state a result similar to Lemma 2.1.

Lemma 2.4. *We consider the real sequence (β_k) defined as in* (11)*, involved in the discretization of the $\partial_t^{\frac{1}{2}}$ operator according to the backward Euler scheme. Let (φ^k) be a complex-valued sequence satisfying $R_{\widehat{\varphi}} < 1$ and $\varphi^0 = 0$. For $N \in \mathbb{N}^*$, we have:*

$$Q_\beta^N \coloneqq \sum_{n=0}^{N-1} \overline{\varphi^{n+1}} \sum_{k=0}^{n+1} \beta_{n+1-k} \varphi^k \quad \in \; S^{\frac{\pi}{4}}. \tag{16}$$

As a consequence, if (φ^k) is a real-valued sequence, we have:

$$\sum_{n=0}^{N-1} \varphi^{n+1} \sum_{k=0}^{n+1} \beta_{n+1-k} \varphi^k \geqslant 0. \tag{17}$$

Proof. Let $N \in \mathbb{N}^*$. Note that we have

$$Q_\beta^N = \sum_{n=0}^{N-1} \overline{\varphi^{n+1}} \sum_{k=0}^{n+1} \beta_{n+1-k} \varphi^k = \sum_{n=0}^{N-1} \overline{\varphi^{n+1}} \left(\beta_k \star \varphi^k \right)_{n+1}.$$

We now write the sum under the form of an infinite sum. Let us define

$$\phi_N^k = \begin{cases} \varphi^k & \text{if } k \leqslant N, \\ 0 & \text{if } k \geqslant N+1, \end{cases}$$

so that

$$Q_\beta^N = \sum_{n=0}^{+\infty} \overline{\phi_N^{n+1}} \left(\beta_k \star \phi_N^k \right)_{n+1} = \sum_{n=0}^{+\infty} \overline{f_n}\, g_n,$$

where we have set

$$f_n = \phi_N^{n+1}, \qquad g_n = \left(\beta_k \star \phi_N^k \right)_{n+1}.$$

The Lemma 2.3 holds, since $R_{\widehat{f}} = 0$. Actually, we have $f_n = 0$ for $n \geqslant N-1$, and thus for all $z \in \mathbb{C}^*$, $\mathcal{Z}(f_n)(z) = \sum_{n=0}^{+\infty} f_n z^{-n}$ is a finite sum, well defined no matter what the value of the nonzero complex z is. So we can write

$$\widehat{f}(z) \coloneqq \mathcal{Z}(f_n)(z) = \mathcal{Z}\left(\phi_N^{n+1}\right)(z) = z\, \mathcal{Z}\left(\phi_N^n\right)(z) = z\, \widehat{\phi_N}(z),$$

using the translation properties of the $\mathcal{Z}$-transform, and the fact that $\phi_N^0 = \varphi^0 = 0$. There is no problem satisfying the hypothesis $R_{\widehat{\phi_N}} < 1$, since $\widehat{\phi_N}(z)$ is a finite sum for all z, whence $R_{\widehat{\phi_N}} = 0$.

We must now determine $R_{\widehat{g}}$ and $\widehat{g}(z)$. Using the translation and convolution properties, the identity $\phi_N^0 = \varphi^0 = 0$, and finally the property $\hat{\beta}(z) = \sqrt{\frac{z-1}{z}}$ (for $|z| > 1$), we have

$$\begin{aligned}
\widehat{g}(z) \coloneqq \mathcal{Z}(g_n)(z) &= \mathcal{Z}\left(\left(\beta_k \star \phi_N^k\right)_{n+1}\right)(z) \\
&= z\,\mathcal{Z}\left(\left(\beta_k \star \phi_N^k\right)_{n}\right)(z) \\
&= z\,\mathcal{Z}\left(\beta_k\right)(z)\,\mathcal{Z}\left(\phi_N^k\right)(z) \\
&= z\sqrt{\frac{z-1}{z}}\,\widehat{\phi_N}(z) = \sqrt{z(z-1)}\,\widehat{\phi_N}(z).
\end{aligned}$$

The function $\widehat{\phi_N}$ is defined for all z different from zero, since as we saw before, its expression is given by a finite sum. The function $z \mapsto \sqrt{z(z-1)}$ is defined for all z. So $\mathcal{Z}(g_n)(z)$ is defined for all nonzero z, and we have $R_{\widehat{g}} = 0$. Thus Lemma 2.3 holds, even when $r = 1$. We then have:

$$\begin{aligned}
Q_\beta^N = \sum_{p=0}^{+\infty} \overline{f_p}\, g_p &= \frac{1}{2\pi}\int_0^{2\pi} \overline{\widehat{f}(e^{i\theta})}\,\widehat{g}(e^{i\theta})\,\mathrm{d}\theta \\
&= \frac{1}{2\pi}\int_0^{2\pi} \left\{ \overline{z\widehat{\phi_N}(z)}\, z\widehat{\phi_N}(z)\sqrt{\frac{z-1}{z}} \right\}\Big|_{z=e^{i\theta}}\,\mathrm{d}\theta \\
&= \frac{1}{2\pi}\int_0^{2\pi} \left\{ \left|z\,\widehat{\phi_N}(z)\right|^2 \sqrt{1-\frac{1}{z}} \right\}\Big|_{z=e^{i\theta}}\,\mathrm{d}\theta \\
&= \frac{1}{2\pi}\int_0^{2\pi} \left|e^{i\theta}\,\widehat{\phi_N}\left(e^{i\theta}\right)\right|^2 \sqrt{1-e^{-i\theta}}\,\mathrm{d}\theta.
\end{aligned}$$

The quantity $\left|e^{i\theta}\widehat{\phi_N}\left(e^{i\theta}\right)\right|^2$ is real-valued and non-negative, so we have only to study the term $\sqrt{1-e^{-i\theta}}$. Yet when θ goes from 0 to 2π, $1-e^{-i\theta}$ sketches the circle of center $z = 1$ and of radius 1, so it remains within the half-plane of non-negative real part. As a consequence, its square root is in the half-cone $S^{\frac{\pi}{4}}$ previously defined. When we integrate, the integral (which equals the sum Q_β^N we are interested in) lies also in $S^{\frac{\pi}{4}}$, hence the result. □

We state below a discrete energy estimate for the formulation (12), which ensures its stability, irrespectively of the values of the mesh size h and of the time step δt.

Proposition 2.5. *The solution to the discrete problem* (12)*, when the source terms f and g are identically equal to zero, verifies, for all $N \geqslant 0$:*

$$\mathcal{E}_h^N + \kappa\,\delta t \sum_{n=0}^{N-1} \|\partial_x u_h^{n+1}\|_{\Omega_\mathrm{F}}^2 \leqslant \mathcal{E}_h^0. \tag{18}$$

Then the scheme (12) *is stable for any value of the discretization parameters h and δt.*

Proof. Once again, the proof follows standard arguments that hold for fully discrete fluid-structure interaction problems, see, e.g., [20], and the main difference comes from the treatment of artificial boundary conditions. Let $\eta_h^{n+1} \in V_\mathrm{S}^{h_\mathrm{S}}$, $\dot{\eta}_h^{n+1} \in V_\mathrm{S}^{h_\mathrm{S}}$ and let $u_h^{n+1} \in V_\mathrm{F}^{h_\mathrm{F}}$ be

the solutions to the discrete problem (12) for source terms f and g identically equal to zero. We have $u_h^{n+1}|_\Sigma = \left(\frac{\eta_h^{n+1}-\eta_h^n}{\delta t}\right)\Big|_\Sigma$. Set

$$\xi_h = \dot\eta_h^{n+\frac12} = \frac{\eta_h^{n+1}-\eta_h^n}{\delta t}, \qquad\qquad v_h = u_h^{n+1}.$$

Thus, we have $\xi_h \in V_{\rm S}^{h_{\rm S}}$, $v_h \in V_{\rm F}^{h_{\rm F}}$, and $\xi_h|_\Sigma = \dot\eta_h^{n+\frac12}|_\Sigma = u_h^{n+1}|_\Sigma = v_h$, and so $(\xi_h, v_h) \in V_{\rm SF}^h$, and the functions ξ_h and v_h thus defined are admissible test functions.

For this choice of test functions, and with vanishing source terms, there holds:

$$\begin{aligned}\int_{\Omega_{\rm S}} \frac{1}{\delta t}(\dot\eta_h^{n+1}-\dot\eta_h^n)\dot\eta_h^{n+\frac12} + \int_{\Omega_{\rm F}} \frac{1}{\delta t}(u_h^{n+1}-u_h^n)u_h^{n+1} + \int_{\Omega_{\rm S}} c^2\,\partial_x\eta_h^{n+\frac12}\partial_x\left(\dot\eta_h^{n+\frac12}\right)\\ + \int_{\Omega_{\rm F}} \kappa\,\partial_x u_h^{n+1}\partial_x u_h^{n+1}\\ = -\int_{\Gamma_{\rm S}} \frac{c}{\delta t}(\eta_h^{n+1}-\eta_h^n)\dot\eta_h^{n+\frac12} - \int_{\Gamma_{\rm F}} \sqrt{\frac{\kappa}{\delta t}}\,u_h^{n+1}\sum_{k=0}^{n+1}\beta_{n+1-k}\,u_h^k.\end{aligned}$$

Using one or the other of the identities $\dot\eta_h^{n+\frac12} = \frac{\dot\eta_h^{n+1}+\dot\eta_h^n}{2}$ or $\dot\eta_h^{n+\frac12} = \frac{\eta_h^{n+1}-\eta_h^n}{\delta t}$, we obtain

$$\begin{aligned}\int_{\Omega_{\rm S}} \frac{\dot\eta_h^{n+1}-\dot\eta_h^n}{\delta t}\frac{\dot\eta_h^{n+1}+\dot\eta_h^n}{2} + \int_{\Omega_{\rm F}} \frac{1}{\delta t}(u_h^{n+1}-u_h^n)u_h^{n+1} + \int_{\Omega_{\rm S}} c^2\,\partial_x\frac{\eta_h^{n+1}+\eta_h^n}{2}\,\partial_x\frac{\eta_h^{n+1}-\eta_h^n}{\delta t}\\ + \int_{\Omega_{\rm F}} \kappa\,\partial_x u_h^{n+1}\partial_x u_h^{n+1}\\ = -\int_{\Gamma_{\rm S}} \frac{c}{\delta t}(\eta_h^{n+1}-\eta_h^n)\frac{1}{\delta t}(\eta_h^{n+1}-\eta_h^n) - \int_{\Gamma_{\rm F}} \sqrt{\frac{\kappa}{\delta t}}\,u_h^{n+1}\sum_{k=0}^{n+1}\beta_{n+1-k}\,u_h^k,\end{aligned}$$

thereby

$$\begin{aligned}\int_{\Omega_{\rm S}} \frac{1}{2\delta t}\left((\dot\eta_h^{n+1})^2-(\dot\eta_h^n)^2\right) + \int_{\Omega_{\rm F}} \frac{1}{\delta t}\left((u_h^{n+1})^2-u_h^n u_h^{n+1}\right) + \int_{\Omega_{\rm S}} \frac{c^2}{2\delta t}\left((\partial_x\eta_h^{n+1})^2-(\partial_x\eta_h^n)^2\right)\\ + \int_{\Omega_{\rm F}} \kappa\,\left(\partial_x u_h^{n+1}\right)^2\\ = -\int_{\Gamma_{\rm S}} \frac{c}{\delta t^2}(\eta_h^{n+1}-\eta_h^n)^2 - \int_{\Gamma_{\rm F}} \sqrt{\frac{\kappa}{\delta t}}\,u_h^{n+1}\sum_{k=0}^{n+1}\beta_{n+1-k}\,u_h^k.\end{aligned}$$

We first deal with the second integral above, which does not immediately appear as one of the energetic quantities we are interested in. However,

$$\begin{aligned}\frac{1}{\delta t}\int_{\Omega_{\rm F}}\left(u_h^{n+1}\right)^2 - \frac{1}{\delta t}\int_{\Omega_{\rm F}} u_h^n u_h^{n+1} &\geqslant \frac{1}{\delta t}\int_{\Omega_{\rm F}}\left(u_h^{n+1}\right)^2 - \frac{1}{\delta t}\left(\int_{\Omega_{\rm F}}(u_h^n)^2\right)^{1/2}\left(\int_{\Omega_{\rm F}}\left(u_h^{n+1}\right)^2\right)^{1/2}\\ &\geqslant \frac{1}{\delta t}\int_{\Omega_{\rm F}}\left(u_h^{n+1}\right)^2 - \frac{1}{2\delta t}\left(\int_{\Omega_{\rm F}}(u_h^n)^2 + \int_{\Omega_{\rm F}}\left(u_h^{n+1}\right)^2\right)\\ &= \frac{1}{2\delta t}\int_{\Omega_{\rm F}}\left(u_h^{n+1}\right)^2 - \frac{1}{2\delta t}\int_{\Omega_{\rm F}}(u_h^n)^2,\end{aligned}$$

using successively the Cauchy-Schwarz inequality and the Young inequality ($ab \leqslant \frac{1}{2}(a^2+b^2)$) on the second term. As a result, there holds

$$\begin{aligned}\frac{1}{2\delta t}\left(\|\dot\eta_h^{n+1}\|_{\Omega_{\rm S}}^2-\|\dot\eta_h^{n}\|_{\Omega_{\rm S}}^2\right)+\frac{1}{2\delta t}\left(c^2\|\partial_x\eta_h^{n+1}\|_{\Omega_{\rm S}}^2-c^2\|\partial_x\eta_h^{n}\|_{\Omega_{\rm S}}^2\right)\\ +\frac{1}{2\delta t}\left(\|u_h^{n+1}\|_{\Omega_{\rm F}}^2-\|u_h^{n}\|_{\Omega_{\rm F}}^2\right)+\kappa\|\partial_x u_h^{n+1}\|_{\Omega_{\rm F}}^2\\ \leqslant -\int_{\Gamma_{\rm S}}\frac{c}{\tau^2}(\eta_h^{n+1}-\eta_h^n)^2-\int_{\Gamma_{\rm F}}\sqrt{\frac{\kappa}{\delta t}}\,u_h^{n+1}\sum_{k=0}^{n+1}\beta_{n+1-k}\,u_h^k.\end{aligned}$$

We now have to prove that the two integrals of the right-hand side are non-negative. As in the continuous case, it is obvious for the first one, and we will use Lemma 2.4 in order to obtain the sign of the second one. Before that, we sum the above relationship from step $n=0$ to step $n=N-1$, for any given $N\in\mathbb{N}^*$. We obtain:

$$\begin{aligned}\frac{1}{2\delta t}\left(\|\dot\eta_h^{N}\|_{\Omega_{\rm S}}^2-\|\dot\eta_h^{0}\|_{\Omega_{\rm S}}^2\right)+\frac{1}{2\delta t}\left(c^2\|\partial_x\eta_h^{N}\|_{\Omega_{\rm S}}^2-c^2\|\partial_x\eta_h^{0}\|_{\Omega_{\rm S}}^2\right)\\ +\frac{1}{2\delta t}\left(\|u_h^{N}\|_{\Omega_{\rm F}}^2-\|u_h^{0}\|_{\Omega_{\rm F}}^2\right)+\sum_{n=0}^{N-1}\kappa\|\partial_x u_h^{n+1}\|_{\Omega_{\rm F}}^2\\ \leqslant -\int_{\Gamma_{\rm S}}\frac{c}{\tau^2}\sum_{n=0}^{N-1}(\eta_h^{n+1}-\eta_h^n)^2-\int_{\Gamma_{\rm F}}\sqrt{\frac{\kappa}{\delta t}}\sum_{n=0}^{N-1}u_h^{n+1}\sum_{k=0}^{n+1}\beta_{n+1-k}\,u_h^k.\end{aligned}$$

Lemma 2.4 ensures that $\displaystyle\sum_{n=0}^{N-1}u_h^{n+1}\sum_{k=0}^{n+1}\beta_{n+1-k}\,u_h^k\geqslant 0$, and thus all the right-hand side is non-positive. Hence the conclusion (18). □

Remark 2.3. Remark that, in the above result, there is an extra dissipation of the energy due to the discrete absorbing boundary conditions, that sums up with the numerical dissipation due to the backward Euler scheme, and the physical dissipation coming from the heat equation.

2.6 Variant with Crank-Nicolson scheme for the heat equation

Instead of using backward Euler for the heat equation, we can use the Crank-Nicolson scheme, and in this case, the essential condition on Σ is then discretized through $u_h^{n+\frac{1}{2}}=\dot\eta_h^{n+\frac{1}{2}}$.

Accordingly, the fully discrete scheme is:

$$\text{Find } \eta_h^{n+1} \in V_{\mathrm{S}}^{h_{\mathrm{S}}},\ \dot\eta_h^{n+1} \in V_{\mathrm{S}}^{h_{\mathrm{S}}} \text{ and } u_h^{n+1} \in V_{\mathrm{F}}^{h_{\mathrm{F}}} \text{ such that:}$$

$$\begin{cases} \displaystyle\int_{\Omega_{\mathrm{S}}} \frac{1}{\delta t}(\dot\eta_h^{n+1} - \dot\eta_h^{n})\xi_h + \int_{\Omega_{\mathrm{F}}} \frac{1}{\delta t}(u_h^{n+1} - u_h^{n})v_h + \int_{\Omega_{\mathrm{S}}} c^2\, \partial_x \eta_h^{n+\frac12} \partial_x \xi_h + \int_{\Omega_{\mathrm{F}}} \kappa\, \partial_x u_h^{n+\frac12} \partial_x v_h \\ \qquad\qquad + \displaystyle\int_{\Gamma_{\mathrm{S}}} \frac{c}{\delta t}(\eta_h^{n+1} - \eta_h^{n})\xi_h + \int_{\Gamma_{\mathrm{F}}} \sqrt{\frac{\kappa}{\tau}} \sum_{k=1}^{n+1} \tilde\beta_{n+1-k}\, u_h^{k-\frac12}\, v_h, \\ \qquad\qquad\qquad\qquad = \displaystyle\int_{\Omega_{\mathrm{S}}} f^{n+\frac12}\xi_h + \int_{\Omega_{\mathrm{F}}} g^{n+\frac12} v_h, \qquad \forall (\xi_h, v_h) \in V_{\mathrm{SF}}^h, \\ \displaystyle\frac{1}{\delta t}(\eta_h^{n+1} - \eta_h^{n}) = u_h^{n+1}, \qquad \text{on } \Sigma, \\ \displaystyle\frac{1}{\delta t}(\eta_h^{n+1} - \eta_h^{n}) = \dot\eta_h^{n+\frac12}, \qquad \text{in } \Omega_{\mathrm{S}}. \end{cases} \tag{19}$$

If we discretize the $\partial_t^{\frac12}$ operator according to Crank-Nicolson scheme, we still obtain a discrete convolution, but with another set of convolution coefficients that we denote by $(\tilde\beta_k)_k$. For this discretization, we have the following lemma, similar to Lemma 2.4.

Lemma 2.6. *We consider the real sequence $(\tilde\beta_k)$ defined by*

$$\sqrt{\frac{1-X}{1+X}} = \sum_{n=0}^{+\infty} \tilde\beta_k\, X^k \quad \textit{for } |X| < 1,$$

involved in the discretization of the $\partial_t^{\frac12}$ operator according to the Crank-Nicolson scheme. Let (φ^k) be a complex-valued sequence satisfying $R_{\widehat\varphi} < 1$ and $\varphi^0 = 0$. For $N \in \mathbb{N}^*$, we have:

$$Q_\beta^N := \sum_{n=0}^{N-1} \overline{\varphi^{n+1}} \sum_{k=0}^{n+1} \tilde\beta_{n+1-k}\varphi^k \quad \in \ S^{\frac\pi4}. \tag{20}$$

As a consequence, if (φ^k) is a real-valued sequence, we have:

$$\sum_{n=0}^{N-1} \varphi^{n+1} \sum_{k=0}^{n+1} \tilde\beta_{n+1-k}\varphi^k \geqslant 0. \tag{21}$$

Using Lemma 2.6 and following the same path as for Proposition 2.5 with minor adaptations, we can prove the stability estimate below for the formulation (19), which ensures also its stability irrespectively of the values of the mesh size h and of the time step δt.

Proposition 2.7. *The solution to the discrete problem* (19)*, when the source terms f and g are identically equal to zero, verifies, for all $N \geqslant 0$:*

$$\mathcal{E}_h^N + \kappa\, \delta t \sum_{n=0}^{N-1} \|\partial_x u_h^{n+1}\|_{\Omega_{\mathrm{F}}}^2 \leqslant \mathcal{E}_h^0. \tag{22}$$

Then the scheme (19) *is stable for any value of the discretization parameters h and δt.*

3 An optimized Schwarz-in-time method

We present in this section an optimized Schwarz-in-time (or Schwarz Waveform Relaxation) method to solve the wave-heat coupled problem (2) described in the previous section. The idea is to solve separately the heat and the wave equations on their respective whole space-time domains, using interface conditions that come from previous computations. Then the new solutions are used to update the interface conditions. Of course, if much iterations are needed to couple the heat and the wave equations, the whole process looses its practical interest, comparatively to a standard method, which consists in solving globally the coupled problem at each time step (as for the monolithic scheme of the previous section). As a result, we need to design carefully the transmission conditions at the interface, so that convergence in a few iterations is expected. To this purpose, we follow the method described in, e.g., [25].

We first present the formal algorithm in a general form, and then focus on the design of optimized conditions.

3.1 The algorithm

We detail here the general principle of the optimized Schwarz-in-time method.

Initialization We compute $\eta^0 \colon (0,T) \times \Omega_S \longrightarrow \mathbb{R}$ and $u^0 \colon (0,T) \times \Omega_F \longrightarrow \mathbb{R}$, respectively solutions to the wave equation on $(0,T) \times \Omega_S$ and to the heat equation on $(0,T) \times \Omega_F$. Each of the two problems is solved independantly of the other. On the external boundary, we still use artificial boundary conditions. On the interface, we use a homogeneous Neumann boundary condition for the wave problem, and a homogeneous Dirichlet boundary condition for the heat problem.

Iteration $k \geqslant 1$ We consider as known the functions $\eta^{k-1} \colon (0,T) \times \Omega_S \longrightarrow \mathbb{R}$ and $u^{k-1} \colon (0,T) \times \Omega_F \longrightarrow \mathbb{R}$.

We compute $\eta^k \colon (0,T) \times \Omega_S \longrightarrow \mathbb{R}$ and $u^k \colon (0,T) \times \Omega_F \longrightarrow \mathbb{R}$ on their respective domains. Each of the two problems is solved independantly of the other. On the external boundary, we still use the artificial boundary conditions. On the interface Σ, we use transmission conditions, designed to accelerate the convergence towards the coupled solution. These transmission conditions depend on the solution in its own domain at the current iteration k, and also on the solution in the neighbouring domain, but at the previous iteration $k-1$ (thus both problems can be solved in parallel).

More precisely, we solve the two following subproblems:

$$\begin{aligned}
&\text{Find } \eta^k \colon (0,T)\times\Omega_{\mathrm{S}} \longrightarrow \mathbb{R} \text{ solution to :}\\
&\begin{cases}
\partial_t^2\eta^k - c^2\,\partial_x^2\eta^k = f, & \text{in } (0,T)\times\Omega_{\mathrm{S}},\\
\eta^k(x,0) = \eta_0(x), & \text{in } (0,T)\times\Omega_{\mathrm{S}},\\
\partial_t\eta^k(x,0) = \dot\eta_0(x), & \text{in } (0,T)\times\Omega_{\mathrm{S}},\\
\partial_{\mathbf{n_S}}\eta^k + \dfrac{1}{c}\,\partial_t\eta^k = 0, & \text{on } (0,T)\times\Gamma_{\mathrm{S}},\\
\phi_S\left(\eta^k, u^{k-1}\right) = 0, & \text{on } (0,T)\times\Sigma.
\end{cases}\\
&\text{Find } u^k \colon (0,T)\times\Omega_{\mathrm{F}} \longrightarrow \mathbb{R} \text{ solution to :}\\
&\begin{cases}
\partial_t u^k - \kappa\,\partial_x^2 u^k = g, & \text{in } (0,T)\times\Omega_{\mathrm{F}},\\
u^k(x,0) = u_0(x), & \text{in } (0,T)\times\Omega_{\mathrm{F}},\\
\partial_{\mathbf{n_F}} u^k + \dfrac{1}{\sqrt{\kappa}}\,\partial_t^{\frac{1}{2}} u^k = 0, & \text{on } (0,T)\times\Gamma_{\mathrm{F}},\\
\phi_F\left(u^k, \eta^{k-1}\right) = 0, & \text{on } (0,T)\times\Sigma.
\end{cases}
\end{aligned} \tag{23}$$

Here, ϕ_S is any function of η^k and u^{k-1}, and of their space or time derivatives at any order; ϕ_F is any function of u^k and η^{k-1}, and of their space or time derivatives at any order.

These functions ϕ_S and ϕ_F must be explicited so as to render optimal the associated transmission conditions

$$\begin{aligned}
&\phi_S\left(\eta^k, u^{k-1}\right) = 0, && \text{on } (0,T)\times\Sigma,\\
&\phi_F\left(u^k, \eta^{k-1}\right) = 0, && \text{on } (0,T)\times\Sigma,
\end{aligned}$$

which means that they guarantee the fastest possible convergence (hopefully a convergence in one or two iterations). Before fixing this issue, we have to establish some properties of the solutions to Problem (23).

3.2 Fourier transform in time

To study the convergence of the above algorithm and to obtain the optimal transmission conditions, we can simply take $f \equiv 0$ et $g \equiv 0$, due to the linearity of the problem. For $f \equiv 0$ and $g \equiv 0$, the solution to Problem (1) is obviously the zero function. We then study the convergence to zero of Algorithm (23).

We consider the time Fourier transform. Here are the notations:

$$\widehat{\eta}(x,\tau) = \mathscr{F}_t(\eta)(x,\tau) \coloneqq \int_{\mathbb{R}^+} \eta(x,t)e^{-it\tau}\,\mathrm{d}t, \qquad \widehat{u}(x,\tau) = \mathscr{F}_t(u)(x,\tau) \coloneqq \int_{\mathbb{R}^+} u(x,t)e^{-it\tau}\,\mathrm{d}t.$$

We consider integrals on $\mathbb{R}^+$ instead of whole $\mathbb{R}$, since all the functions we deal with are equal to zero for negative times.

We apply the time Fourier transform to the wave equation in (23). Given that $f \equiv 0$, we obtain:

$$-\tau^2\widehat{\eta^k}(x,\tau) - c^2\partial_x^2\widehat{\eta^k}(x,\tau) = 0, \qquad x \in \Omega_{\mathrm{S}},$$

that we rewrite

$$\partial_x^2 \widehat{\eta^k}(x,\tau) + \left(\frac{\tau}{c}\right)^2 \widehat{\eta^k}(x,\tau) = 0, \qquad x \in \Omega_{\rm S}.$$

This is an ordinary differential equation of order two in x, whose general solutions are given by

$$\widehat{\eta^k}(x,\tau) = A(\tau) e^{i\frac{\tau}{c}x} + B(\tau) e^{-i\frac{\tau}{c}x}, \qquad x \in \Omega_{\rm S}. \tag{24}$$

On the other hand, we consider the time Fourier transform of the artificial boundary condition satisfied by the solution of the wave problem on the external boundary $\Gamma_{\rm S}$:

$$\partial_{\mathbf{n_S}} \widehat{\eta^k}(x,\tau) + i\,\frac{\tau}{c}\,\widehat{\eta^k}(x,\tau) = 0, \qquad x \in \Gamma_{\rm S}.$$

On the external boundary $\Gamma_{\rm S} = \{-x_S\}$, we have $\partial_{\mathbf{n_S}}|_{\Gamma_{\rm S}} = -\partial_x|_{\Gamma_{\rm S}}$, whence, substituting the expression obtained in (24) into the above equation:

$$-i\,\frac{\tau}{c}\,A(\tau)e^{i\frac{\tau}{c}x} + i\,\frac{\tau}{c}\,B(\tau)e^{-i\frac{\tau}{c}x} + i\,\frac{\tau}{c}\left(A(\tau)e^{i\frac{\tau}{c}x} + B(\tau)e^{-i\frac{\tau}{c}x}\right) = 0, \qquad x \in \Omega_{\rm S},$$

and then

$$2i\,\frac{\tau}{c}\,B(\tau)e^{i\frac{\tau}{c}x} = 0, \qquad x \in \Omega_{\rm S}.$$

We deduce that the term $B(\tau)$ is equal to zero, for all τ. So the expression (24) becomes:

$$\widehat{\eta^k}(x,\tau) = A(\tau)e^{i\frac{\tau}{c}x}, \qquad x \in \Omega_{\rm S},$$

and then

$$\widehat{\eta^k}(x,\tau) = \widehat{\eta^k}(0,\tau)\, e^{i\frac{\tau}{c}x}, \qquad x \in \Omega_{\rm S}. \tag{25}$$

Consequently, we also obtain the expression of $\partial_x \widehat{\eta^k}(x,\tau)$:

$$\partial_x \widehat{\eta^k}(x,\tau) = i\,\frac{\tau}{c}\,\widehat{\eta^k}(x,\tau), \qquad x \in \Omega_{\rm S}. \tag{26}$$

Now this expression is valid on whole domain $\Omega_{\rm S}$, and not only on $\Gamma_{\rm S}$.

We now apply the same process to the heat equation in (23). Using that $g \equiv 0$, the time Fourier transform gives:

$$i\tau\,\widehat{u^k}(x,\tau) - \kappa\partial_x^2 \widehat{u^k}(x,\tau) = 0, \qquad x \in \Omega_{\rm F},$$

that is

$$\partial_x^2 \widehat{u^k}(x,\tau) - i\,\frac{\tau}{\kappa}\,\widehat{u^k}(x,\tau) = 0, \qquad x \in \Omega_{\rm F}.$$

This is an ordinary differential equation of order two in x, whose general solutions are given by

$$\widehat{u^k}(x,\tau) = A(\tau)e^{\sqrt{i\frac{\tau}{\kappa}}x} + B(\tau)e^{-\sqrt{i\frac{\tau}{\kappa}}x}, \qquad x \in \Omega_{\rm F}. \tag{27}$$

On the other hand, we consider the time Fourier transform of the artificial boundary condition satisfied by the solution of the heat problem on the external boundary $\Gamma_{\rm F}$:

$$\partial_{\mathbf{n_F}} \widehat{u^k}(x,\tau) + \sqrt{i\,\frac{\tau}{\kappa}}\,\widehat{u^k}(x,\tau) = 0, \qquad x \in \Gamma_{\rm F}.$$

On the external boundary $\Gamma_{\rm F} = \{x_F\}$, we have $\partial_{\mathbf{n_F}}|_{\Gamma_{\rm F}} = \partial_x|_{\Gamma_{\rm F}}$, whence, substituting the expression obtained in (27) into the above equation:

$$\sqrt{i\frac{\tau}{\kappa}}\,A(\tau)e^{\sqrt{i\frac{\tau}{\kappa}}\,x} - \sqrt{i\frac{\tau}{\kappa}}\,B(\tau)e^{-\sqrt{i\frac{\tau}{\kappa}}\,x} + \sqrt{i\frac{\tau}{\kappa}}\left(A(\tau)e^{\sqrt{i\frac{\tau}{\kappa}}\,x} + B(\tau)e^{-\sqrt{i\frac{\tau}{\kappa}}\,x}\right) = 0,\ x \in \Omega_{\rm F},$$

and then

$$2\sqrt{i\frac{\tau}{\kappa}}\,A(\tau)e^{\sqrt{i\frac{\tau}{\kappa}}\,x} = 0, \qquad x \in \Omega_{\rm F}.$$

We deduce that the term $A(\tau)$ is equal to zero, for all τ. So the expression (27) becomes:

$$\widehat{u^k}(x,\tau) = B(\tau)e^{-\sqrt{i\frac{\tau}{\kappa}}\,x}, \qquad x \in \Omega_{\rm F},$$

and then

$$\widehat{u^k}(x,\tau) = \widehat{u^k}(0,\tau)e^{-\sqrt{i\frac{\tau}{\kappa}}\,x}, \qquad x \in \Omega_{\rm F}. \tag{28}$$

Consequently, we also obtain the expression of $\partial_x\widehat{u^k}(x,\tau)$:

$$\partial_x\widehat{u^k}(x,\tau) = -\sqrt{i\frac{\tau}{\kappa}}\,\widehat{u^k}(x,\tau), \qquad x \in \Omega_{\rm F}. \tag{29}$$

Now this expression is valid on whole domain $\Omega_{\rm F}$, and not only on $\Gamma_{\rm F}$.

3.3 Optimal transmission conditions

In this section, we state the main result of this paper, which is the obtention of optimal transmission conditions for the 1D wave-heat coupled problem (1). We design transmission conditions according to the physical interface conditions; namely we want to recover, when $k \to +\infty$, the interface conditions (i) and (ii) of Problem (1). A simple choice consists in writing:

$$\left(S_1\partial_t + c^2\partial_x\right)\eta^k|_\Sigma = \left(S_1 + \kappa\partial_x\right)u^{k-1}|_\Sigma, \tag{30}$$

$$\left(S_2 + \kappa\partial_x\right)u^k|_\Sigma = \left(S_2\partial_t + c^2\partial_x\right)\eta^{k-1}|_\Sigma, \tag{31}$$

with S_1 and S_2 two pseudodifferential operators in time, of respective symbols s_1 and s_2. This choice allows to recover, to the limit, the wave-heat coupling conditions. Indeed, if we assume that Algorithm (23) converges, and denoting by η^* and u^* the solutions obtained when $k \to +\infty$, we get at the limit:

$$\begin{aligned}\left(S_1\partial_t + c^2\partial_x\right)\eta^*|_\Sigma &= \left(S_1 + \kappa\partial_x\right)u^*|_\Sigma,\\ \left(S_2 + \kappa\partial_x\right)u^*|_\Sigma &= \left(S_2\partial_t + c^2\partial_x\right)\eta^*|_\Sigma.\end{aligned} \tag{32}$$

Adding up the two equalities yields:

$$(S_1 - S_2)\partial_t\eta^*|_\Sigma = (S_1 - S_2)u^*|_\Sigma.$$

Assuming that $(S_1 - S_2)$ is injective, we check that $\partial_t\eta^*|_\Sigma = u^*|_\Sigma$, that is (1) (i). Reporting then the equation (1) (i) into one of the equalities of (32), we get (1) (ii).

In this context, we can state the following result:

Theorem 3.1. *Set $f \equiv 0$ and $g \equiv 0$, and, for $k \geqslant 1$, denote by $\widehat{\eta^k}$ and $\widehat{u^k}$ the respective solutions of Algorithm* (23) *in the time Fourier domain, when conditions* (30)–(31) *are applied. Then there holds*

$$\widehat{\eta^k} = \rho_1(\tau)\,\widehat{u^{k-1}}, \quad \widehat{u^k} = \rho_2(\tau)\,\widehat{\eta^{k-1}}, \tag{33}$$

with the following expressions for the convergence factors

$$\rho_1(\tau) = \frac{s_1 - \sqrt{i\tau\kappa}}{i\tau(s_1 + c)} \qquad \text{and} \qquad \rho_2(\tau) = \frac{i\tau(s_2 + c)}{s_2 - \sqrt{i\tau\kappa}}. \tag{34}$$

So the global convergence factor $\rho = \rho_1\rho_2$ is

$$\rho(\tau) = \frac{s_1 - \sqrt{i\tau\kappa}}{s_1 + c}\,\frac{s_2 + c}{s_2 - \sqrt{i\tau\kappa}}. \tag{35}$$

Then there holds

$$\widehat{\eta^{2k}} = \rho(\tau)\,\widehat{\eta^{2k-2}}, \quad \widehat{u^{2k}} = \rho(\tau)\,\widehat{u^{2k-2}}.$$

Proof. In the time Fourier domain, conditions (30)–(31) become:

$$\begin{aligned}
\left(s_1 i\tau + c^2\partial_x\right)\widehat{\eta^k} &= \left(s_1 + \kappa\partial_x\right)\widehat{u^{k-1}},\\
\left(s_2 + \kappa\partial_x\right)\widehat{u^k} &= \left(s_2 i\tau + c^2\partial_x\right)\widehat{\eta^{k-1}}.
\end{aligned}$$

We then rewrite these conditions, using the expression of $\partial_x\widehat{\eta^k}$ as a function of $\widehat{\eta^k}$, and that of $\partial_x\widehat{u^k}$ as a function of $\widehat{u^k}$ (these expressions have been obtained in (26) and (29)). For the first equation, we get:

$$\begin{aligned}
\left(s_1 i\tau + i\frac{\tau}{c}\,c^2\right)\widehat{\eta^k} &= \left(s_1 - \sqrt{i\frac{\tau}{\kappa}\kappa}\right)\widehat{u^{k-1}},\\
\widehat{\eta^k} &= \frac{s_1 - \sqrt{i\tau\kappa}}{i\tau(s_1 + c)}\,\widehat{u^{k-1}},
\end{aligned}$$

and for the second equation, we get similarly:

$$\begin{aligned}
\left(s_2 - \sqrt{i\frac{\tau}{\kappa}\kappa}\right)\widehat{u^k} &= \left(s_2 i\tau + i\frac{\tau}{c}\,c^2\right)\widehat{\eta^{k-1}},\\
\widehat{u^k} &= \frac{i\tau(s_2 + c)}{s_2 - \sqrt{i\tau\kappa}}\,\widehat{\eta^{k-1}}.
\end{aligned}$$

Therefore we obtain relationships (33) and (34). It just suffices to gather the two above results (at iterations k and $k-1$, respectively) to obtain the expression (35) for the convergence rate. □

From the above result, we obtain the expression of the optimal conditions for the Schwarz-in-time method.

Corollary 3.2. *The optimal conditions for Algorithm* (23)*, for which both convergence factors* ρ_1 *and* ρ_2 *vanish, are:*

$$s_1^\star = \sqrt{i\tau\kappa} \qquad \textit{and} \qquad s_2^\star = -c, \tag{36}$$

and they correspond to the operators

$$S_1^\star = \sqrt{\kappa}\,\partial_t^{\frac{1}{2}} \qquad \textit{and} \qquad S_2^\star = -c. \tag{37}$$

Note that for these choices the denominators do not vanish, the cancellation condition being $\sqrt{\kappa}\sqrt{i\tau} \neq -c$. We finally get the following optimal transmission conditions:

$$\begin{cases} \left(\sqrt{\kappa}\partial_t^{\frac{3}{2}} + c^2\partial_x\right)\eta^k|_\Sigma = \left(\sqrt{\kappa}\partial_t^{\frac{1}{2}} + \kappa\partial_x\right)u^{k-1}|_\Sigma, \\ (-c+\kappa\partial_x)\,u^k|_\Sigma = \left(-c\,\partial_t + c^2\partial_x\right)\eta^{k-1}|_\Sigma. \end{cases} \tag{38}$$

Of course, if these conditions are implemented, both ρ_1 and ρ_2 vanish and convergence is obtained in at most one iteration, irrespectively of the value of the initial conditions.

Note that the optimal condition associated to the symbol s_2 leads to a local operator of order zero, $S_2^\star = -c$, so there is no need to approximate it. However it is not the same with the condition associated to the symbol s_1. Indeed, the choice $s_1 = \sqrt{\kappa}\sqrt{i\tau}$ leads to a nonlocal operator $\sqrt{\kappa}\,\partial_t^{\frac{1}{2}}$, source of increased numerical complexity. In practice, for a simple method, we can approximate S_1 by a local operator $\widetilde{S_1}$, for instance a constant operator. Remark that for $S_1 \neq S_1^\star$, convergence is expected in two iterations instead of one.

3.4 The fully discrete Schwarz-in-time method

For the implementation, we simply choose constants for the operators S_1 and S_2, that will be denoted still by s_1 and s_2. This will allow to test the behaviour of the algorithm for different values of these constants.

So the Schwarz-in-time algorithm can be rewritten as follows, for $k \in \mathbb{N}^*$, knowing η^{k-1} and u^{k-1}.

Find $\eta^k \colon (0,T)\times\Omega_{\rm S} \longrightarrow \mathbb{R}$ solution to:

$$\begin{cases} \partial_t^2\eta^k - c^2\,\partial_x^2\eta^k = f, & \text{in } (0,T)\times\Omega_{\rm S}, \\ \eta^k(x,0) = \eta_0(x), & \text{in } \Omega_{\rm S}, \\ \partial_t\eta^k(x,0) = \dot\eta_0(x), & \text{in } \Omega_{\rm S}, \\ \partial_{\mathbf{n_S}}\eta^k + \dfrac{1}{c}\,\partial_t\eta^k = 0, & \text{on } (0,T)\times\Gamma_{\rm S}, \\ \left(s_1\partial_t + c^2\partial_{\mathbf{n_S}}\right)\eta^k = (s_1 - \kappa\partial_{\mathbf{n_F}})\,u^{k-1}, & \text{on } (0,T)\times\Sigma. \end{cases} \tag{39}$$

Find $u^k \colon (0,T)\times\Omega_{\rm F} \longrightarrow \mathbb{R}$ solution to:

$$\begin{cases} \partial_t u^k - \kappa\,\partial_x^2 u^k = g, & \text{in } (0,T)\times\Omega_{\rm F}, \\ u^k(x,0) = u_0(x), & \text{in } \Omega_{\rm F}, \\ \partial_{\mathbf{n_F}}u^k + \dfrac{1}{\sqrt{\kappa}}\,\partial_t^{\frac{1}{2}}u^k = 0, & \text{on } (0,T)\times\Gamma_{\rm F}, \\ (s_2 - \kappa\partial_{\mathbf{n_F}})\,u^k = \left(s_2\partial_t + c^2\partial_{\mathbf{n_S}}\right)\eta^{k-1}, & \text{on } (0,T)\times\Sigma. \end{cases}$$

Let us derive the weak formulation associated to Problem (39). We first write the two subproblems without taking into account the different conditions on the external boundary and on the interface Σ:

Find, for $t > 0$, $\eta^k(t) \in V_{\mathrm{S}}$ such that:

$$\begin{cases} \dfrac{d^2}{dt^2} \displaystyle\int_{\Omega_{\mathrm{S}}} \eta^k(t)\xi + \int_{\Omega_{\mathrm{S}}} c^2\, \partial_x \eta^k(t) \partial_x \xi - \int_{\Gamma_{\mathrm{S}}} c^2\, \partial_{\mathbf{n_S}} \eta^k(t)\xi - \int_{\Sigma} c^2\, \partial_{\mathbf{n_S}} \eta^k(t)\xi \\ \qquad\qquad = \displaystyle\int_{\Omega_{\mathrm{S}}} f(t)\xi, \qquad \forall \xi \in V_{\mathrm{S}}, \end{cases}$$

Find, for $t > 0$, $u^k(t) \in V_{\mathrm{F}}$ such that:

$$\begin{cases} \dfrac{d}{dt} \displaystyle\int_{\Omega_{\mathrm{F}}} u^k(t) v + \int_{\Omega_{\mathrm{F}}} \kappa\, \partial_x u^k(t) \partial_x v - \int_{\Gamma_{\mathrm{F}}} \kappa\, \partial_{\mathbf{n_F}} u^k(t) v - \int_{\Sigma} \kappa\, \partial_{\mathbf{n_F}} u^k(t) v \\ \qquad\qquad = \displaystyle\int_{\Omega_{\mathrm{F}}} g(t) v, \qquad \forall v \in V_{\mathrm{F}}. \end{cases}$$

We now incorporate the boundary and interface conditions: we replace the boundary terms on Γ_{S} and Γ_{F} for one part, and on Σ for another part, using the artificial boundary conditions and the transmission conditions respectively. More precisely, we have:

$$\begin{aligned} c^2 \partial_{\mathbf{n_S}} \eta^k(t)|_{\Gamma_{\mathrm{S}}} &= -\, c\, \partial_t \eta^k(t)|_{\Gamma_{\mathrm{S}}}, \\ c^2 \partial_{\mathbf{n_S}} \eta^k(t)|_{\Sigma} &= -\, s_1 \partial_t \eta^k(t)|_{\Sigma} + (s_1 - \kappa \partial_{\mathbf{n_F}})\, u^{K-1}|_{\Sigma}, \\ -\kappa \partial_{\mathbf{n_F}} u^k(t)|_{\Gamma_{\mathrm{F}}} &= \sqrt{\kappa}\, \partial_t^{\frac{1}{2}} u^k(t)|_{\Gamma_{\mathrm{F}}}, \\ -\kappa \partial_{\mathbf{n_F}} u^k(t)|_{\Sigma} &= -\, s_2 u^k(t)|_{\Sigma} + \left(s_2 \partial_t + c^2 \partial_{\mathbf{n_S}}\right) \eta^{k-1}|_{\Sigma}. \end{aligned}$$

We then obtain:

$$\begin{cases} \displaystyle\int_{\Omega_{\mathrm{S}}} \partial_t^2 \eta^k(t)\xi + \int_{\Omega_{\mathrm{S}}} c^2\, \partial_x \eta^k(t) \partial_x \xi + \int_{\Gamma_{\mathrm{S}}} c\, \partial_t \eta^k(t)\xi + \int_{\Sigma} s_1 \partial_t \eta^k(t)\xi \\ \qquad = \displaystyle\int_{\Sigma} s_1 u^{k-1}(t)\xi - \int_{\Sigma} \kappa\, \partial_{\mathbf{n_F}} u^{k-1}(t)\xi + \int_{\Omega_{\mathrm{S}}} f(t)\xi,\ \forall \xi \in V_{\mathrm{S}}. \end{cases}$$

Find, for $t > 0$, $u^k(t) \in V_{\mathrm{F}}$ such that:

$$\begin{cases} \displaystyle\int_{\Omega_{\mathrm{F}}} \partial_t u^k(t) v + \int_{\Omega_{\mathrm{F}}} \kappa\, \partial_x u^k(t) \partial_x v + \int_{\Gamma_{\mathrm{F}}} \sqrt{\kappa}\, \partial_t^{\frac{1}{2}} u^k(t) v - \int_{\Sigma} s_2\, u^k(t) v \\ \qquad = -\displaystyle\int_{\Sigma} s_2\, \partial_t \eta^{k-1}(t) v - \int_{\Sigma} c^2 \partial_{\mathbf{n_S}} \eta^{k-1}(t) v + \int_{\Omega_{\mathrm{F}}} g(t) v,\ \forall v \in V_{\mathrm{F}}. \end{cases} \tag{40}$$

The space discretization is done as before, using the finite element spaces

$$V_{\mathrm{S}}^{h_{\mathrm{S}}} \coloneqq \langle \varphi_1^S, \ldots, \varphi_N^S \rangle, \qquad\qquad V_{\mathrm{F}}^{h_{\mathrm{F}}} \coloneqq \langle \varphi_1^F, \ldots, \varphi_M^F \rangle.$$

Note that h_{S} and h_{F} may be the same.

The fully discrete problem, still with Crank-Nicolson for the wave, and backward Euler

for the heat, reads:

Find, for $n \in \mathbb{N}$, $\eta_h^{k,n+1}$ and $\dot{\eta}_h^{k,n+1} \in V_{\mathrm{S}}^{h_{\mathrm{S}}}$ such that:

$$\begin{cases} \displaystyle\int_{\Omega_{\mathrm{S}}} \frac{\dot{\eta}_h^{k,n+1} - \dot{\eta}_h^{k,n}}{\delta t}\xi_h + \int_{\Omega_{\mathrm{S}}} c^2\, \partial_x \eta_h^{k,n+\frac{1}{2}} \partial_x \xi_h + \int_{\Gamma_{\mathrm{S}}} c\, \frac{\eta_h^{k,n+1} - \eta_h^{k,n}}{\delta t}\xi_h \\ \displaystyle + \int_{\Sigma} s_1 \frac{\eta_h^{k,n+1} - \eta_h^{k,n}}{\delta t}\xi_h \\ \displaystyle = \int_{\Sigma} s_1\, u_h^{k-1,n+1}\xi_h - \int_{\Sigma} \kappa \partial_{\mathbf{n_F}} u_h^{k-1,n+1}\xi_h \\ \displaystyle + \int_{\Omega_{\mathrm{S}}} f^{n+\frac{1}{2}}\xi_h, \qquad \forall \xi_h \in V_{\mathrm{S}}^{h_{\mathrm{S}}}, \\ \dot{\eta}_h^{k,n+\frac{1}{2}} = \dfrac{\eta_h^{k,n+1} - \eta_h^{k,n}}{\delta t}, \quad \text{in } \Omega_{\mathrm{S}}. \end{cases} \tag{41}$$

Find, for $n \in \mathbb{N}$, $u_h^{k,n+1} \in V_{\mathrm{F}}^{h_{\mathrm{F}}}$ such that:

$$\begin{cases} \displaystyle\int_{\Omega_{\mathrm{F}}} \frac{u_h^{k,n+1} - u_h^{k,n}}{\delta t} v_h + \int_{\Omega_{\mathrm{F}}} \kappa\, \partial_x u_h^{k,n+1} \partial_x v_h + \sqrt{\frac{\kappa}{\delta t}} \int_{\Gamma_{\mathrm{F}}} u_h^{k,n+1} v_h - \int_{\Sigma} s_2\, u_h^{k,n+1} v_h \\ \displaystyle = -\int_{\Sigma} s_2\, \frac{\eta_h^{k-1,n+1} - \eta_h^{k-1,n}}{\delta t} v_h - \int_{\Sigma} c^2 \partial_{\mathbf{n_S}} \eta_h^{k-1,n+\frac{1}{2}} v_h \\ \displaystyle - \sqrt{\frac{\kappa}{\delta t}} \sum_{p=0}^{n} \beta_{n+1-p} \int_{\Gamma_{\mathrm{F}}} u_h^{k,p} v_h + \int_{\Omega_{\mathrm{F}}} g^{n+1} v_h, \qquad \forall v_h \in V_{\mathrm{F}}^{h_{\mathrm{F}}}. \end{cases}$$

Here, the fractional derivative of half order has been discretized using the discrete convolution, with coefficients adapted to the backward Euler scheme.

4 Numerical experiments

For the numerical simulations, we take $\Omega_S = (-1, 0)$ and $\Omega_F = (0, 1)$. We consider a gaussian initial datum for η_0 in the wave domain, and the zero function for u_0 in the heat domain and $\dot{\eta}_0$ in the wave domain:

$$\begin{aligned} &\eta_0(x) = e^{-50\left(x+\frac{1}{2}\right)^2}, && \text{in } \Omega_S, \\ &\dot{\eta}_0(x) = 0, && \text{in } \Omega_S, \\ &u_0(x) = 0, && \text{in } \Omega_F. \end{aligned} \tag{42}$$

These initial data are represented on Figure 2(a). Furthermore, we consider the source terms f and g identically equal to zero.

4.1 Comparison to the reference solution

As a reference solution, we consider the solution computed using the monolithic algorithm (12). The parameters are $c = 3$ for the wave equation and $\kappa = 1$ for the heat equation. The time step is $\delta t = 5 \cdot 10^{-3}$, and we consider $N_S = 81$ and $N_F = 80$ points for the space discretization in the wave and heat domains respectively. The evolution of the

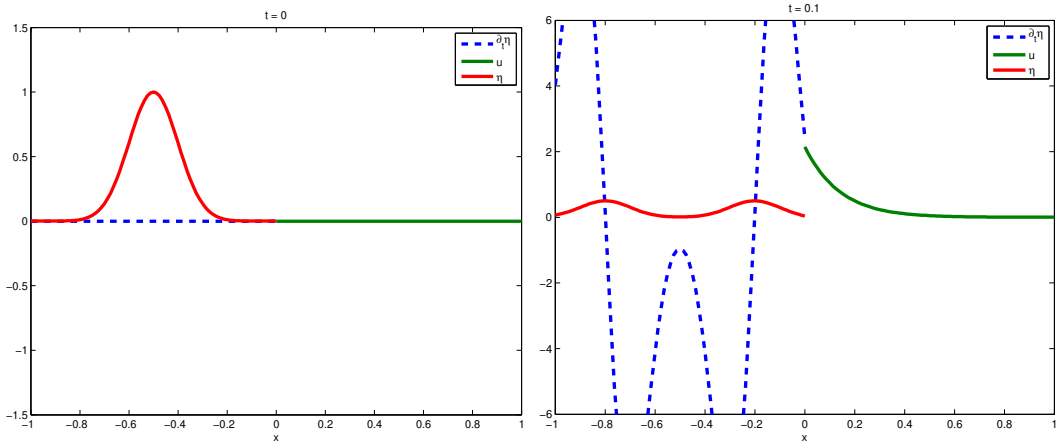

(a) $t = 0$ (b) $t = 0.1$

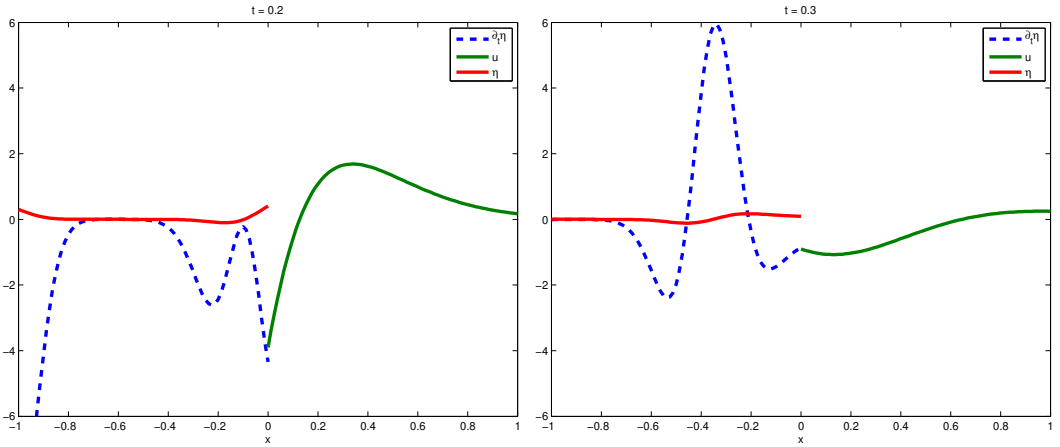

(c) $t = 0.2$ (d) $t = 0.3$

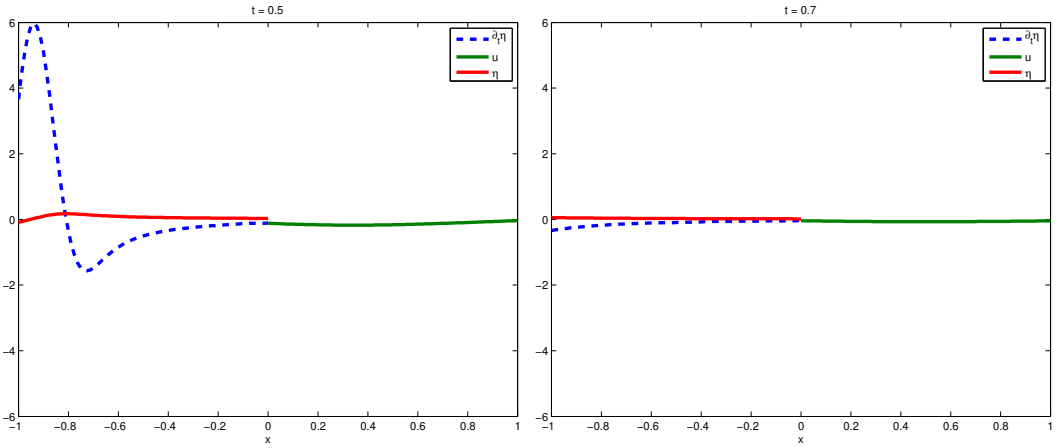

(e) $t = 0.5$ (f) $t = 0.7$

Figure 2: Reference solution obtained with the monolithic algorithm, for $c = 3$ and $\kappa = 1$, at various times of the computation.

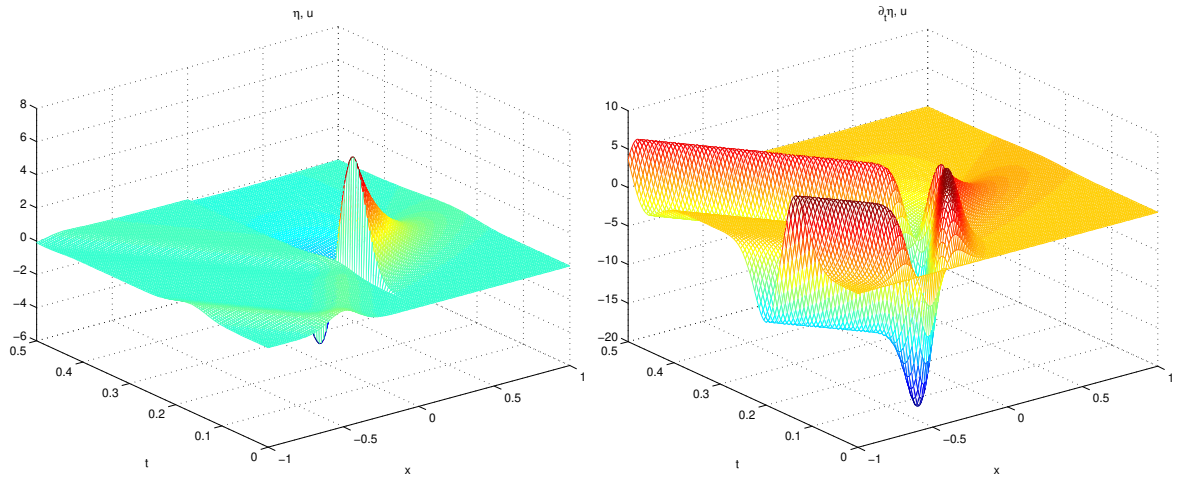

(a) η in Ω_S, u in Ω_F (b) $\partial_t\eta$ in Ω_S, u in Ω_F

Figure 3: Reference solution obtained with the monolithic algorithm, for $c = 3$ and $\kappa = 1$, up to $T = 0.5$.

solution until the final time of computation $T = 0.5$ is given Figure 2. Figure 3 depicts a three-dimensional representation of this solution.

We need to study the efficiency of Algorithm (41) (Schwarz-in-time / waveform relaxation) compared to the monolithic algorithm (12). The optimized algorithm depends on three parameters: the total number of Schwarz iterations, that we denote by K, and the parameters s_1 and s_2 which approximate the symbols of the optimal operators S_1 and S_2.

For a set of parameters, for instance $K = 4$, $s_1 = 1$ and $s_2 = -3$, we plot the evolution in time of the functions η, u and $\partial_t\eta$ at the midpoint of their respective intervals. For the discretization $\delta t = 10^{-2}$, $N_S = 41$, $N_F = 40$, a final time $T = 1$, and still $c = 3$ and $\kappa = 1$, we obtain the results shown on Figures 4(a), 4(b) and 4(c). We can see that both curves match accurately. We also plot on Figure 4(d) the evolution in time of the discrete energy of the coupled system, given by (13). In accordance with Proposition 2.5, we observe that the energy is decreasing over the time. This is still the case for other values of c. For instance, for $c = 1$ the decrease of the energy is slower, but the result is of similar accuracy.

We now require a quantitative estimate in order to measure the accuracy of the algorithm. To this end, we consider two discrete norms, ℓ^2 and ℓ^∞. First, let us define the error between the monolithic and the Schwarz-in-time solutions. We consider the solution given by the monolithic algorithm as a reference solution, and compare the result given by Algorithm (41) to this reference. More precisely, we define the error on each of the three functions η, $\dot\eta$ and u:

$$\begin{aligned} e^n_{h,\eta} &:= \eta^{K,n}_{h,\text{relaxation}} - \eta^n_{h,\text{monolithic}} &&\in V_{\text{S}}^{h_{\text{S}}}, \\ e^n_{h,\dot\eta} &:= \dot\eta^{K,n}_{h,\text{relaxation}} - \dot\eta^n_{h,\text{monolithic}} &&\in V_{\text{S}}^{h_{\text{S}}}, \\ e^n_{h,u} &:= u^{K,n}_{h,\text{relaxation}} - u^n_{h,\text{monolithic}} &&\in V_{\text{F}}^{h_{\text{F}}}. \end{aligned} \tag{43}$$

at a given time t^n and after K iterations of the relaxation algorithm (41), and

$$e_{h,f} := \left(e^n_{h,f}\right)_{0\leqslant n\leqslant N}, \qquad f \in \{\eta, \dot\eta, u\}.$$

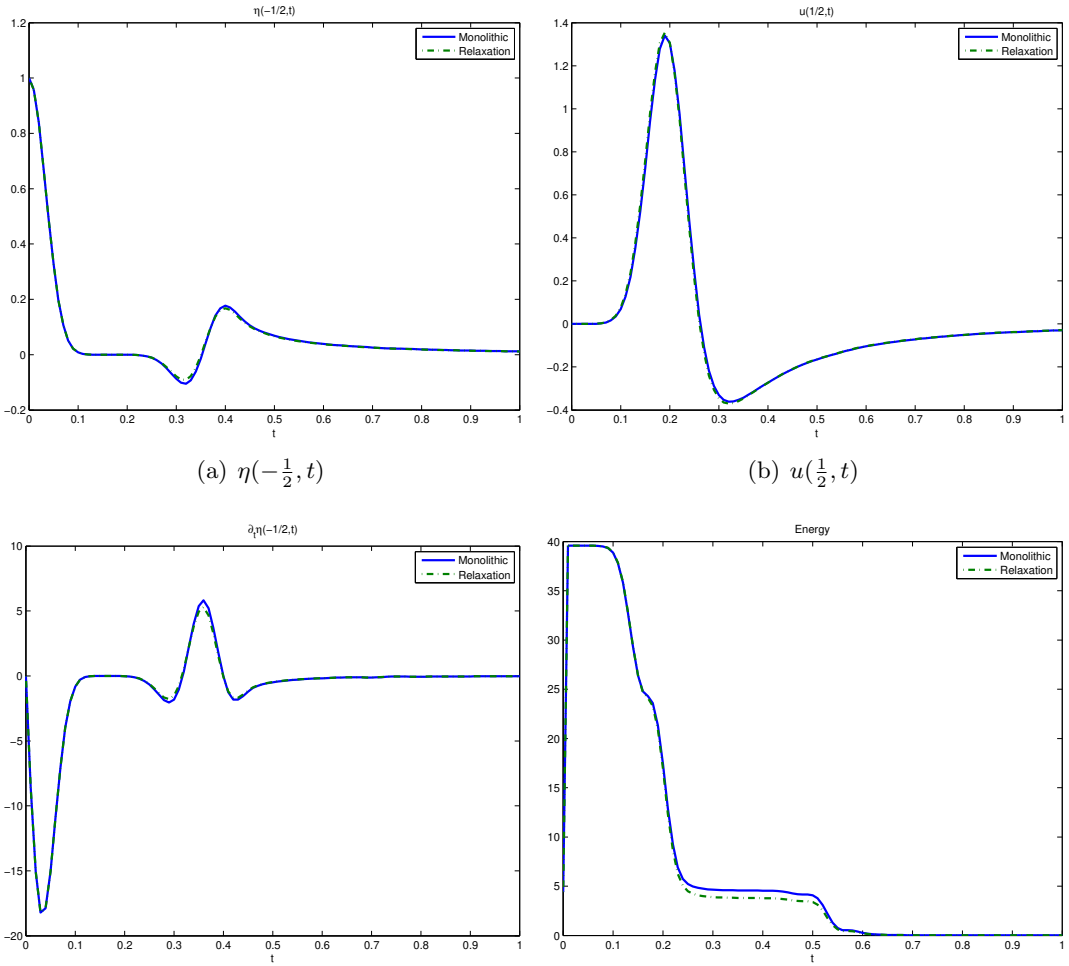

(a) $\eta(-\frac{1}{2}, t)$ (b) $u(\frac{1}{2}, t)$

(c) $\partial_t \eta(-\frac{1}{2}, t)$ (d) Energy $\mathcal{E}_h(t)$

Figure 4: η, u, and $\partial_t \eta$ at the midpoint of their respective intervals, and energy of the system, with respect to time.

Now for $f \in \{\eta, \dot{\eta}, u\}$, and V being $V_{\mathrm{S}}^{h_{\mathrm{S}}}$ or $V_{\mathrm{F}}^{h_{\mathrm{F}}}$ as the case may be, we define:

$$\|e_{h,f}\|^2_{\ell^2([t^0,t^N],V)} := \delta t \sum_{n=0}^{N} \|e^n_{h,f}\|^2_{L^2(V)}, \tag{44}$$

$$\|e_{h,f}\|_{\ell^\infty([t^0,t^N],V)} := \max_{0\leqslant n\leqslant N} \|e^n_{h,f}\|_{L^2(V)}, \tag{45}$$

and finally:

$$\begin{aligned} \|e_h\|^2_{\ell^2} &:= \|e_{h,\eta}\|^2_{\ell^2([t^0,t^N],V_{\mathrm{S}}^{h_{\mathrm{S}}})} + \|e_{h,\dot{\eta}}\|^2_{\ell^2([t^0,t^N],V_{\mathrm{S}}^{h_{\mathrm{S}}})} + \|e_{h,u}\|^2_{\ell^2([t^0,t^N],V_{\mathrm{F}}^{h_{\mathrm{F}}})}, \\ \|e_h\|_{\ell^\infty} &:= \max\left(\|e_{h,\eta}\|_{\ell^\infty([t^0,t^N],V_{\mathrm{S}}^{h_{\mathrm{S}}})}; \|e_{h,\dot{\eta}}\|_{\ell^\infty([t^0,t^N],V_{\mathrm{S}}^{h_{\mathrm{S}}})}; \|e_{h,u}\|_{\ell^\infty([t^0,t^N],V_{\mathrm{F}}^{h_{\mathrm{F}}})}\right). \end{aligned} \tag{46}$$

For instance, the simulations shown on Figure 4 for $c = 3$ and $T = 1$ give $\|e_h\|_{\ell^2} = 0.0247$ and $\|e_h\|_{\ell^\infty} = 0.0446$.

We are going to use these two discrete norms to study the influence of the parameters on Algorithm (41). For a given discretization and a given set of parameters, we represent the ℓ^2 and ℓ^∞ norms of the error, according to one of the parameters.

4.2 Influence of the total number of Schwarz iterations

Let us recall that K denotes the total number of Schwarz iterations in Algorithm (41). Theoretically with the optimal choice $s_2 = -c$ the algorithm converges in two iterations, so we could consider $K = 2$. Yet in practice there are numerical errors, so one must consider a bit more iterations; but not much more. Figure 5 shows that $K = 4$ is a good compromise between the time of computation and the precision of the simulation, and this result does not depend of either space or time discretization. In these simulations we have taken $c = 3$, $\kappa = 1$, $T = 2$, $s_1 = 2$ and $s_2 = -c$. We can also notice that making too many iterations is useless as far as precision is concerned, but in the same time it does not degrade the result either.

Henceforth we consider $K = 4$ iterations of the relaxation algorithm in all further computations, and the following discretization parameters: $\delta t = 10^{-2}$, $N_S = 41$, $N_F = 40$. The parameter κ will be fixed at $\kappa = 1$, whereas c may vary. Thus, we are now to study the influence of the relaxation parameters s_1 and s_2, for different values of c.

4.3 Influence of the parameter s_2

We now study the influence of s_2 on the optimized Schwarz algorithm (41). There is no approximation to be done on the optimal operator $S_2^\star$ which is the constant operator $S_2^\star = -c$. As a result, we expect the choice $s_2^\star = -c$ to be optimal also in numerical simulations, independently of the choice of c or s_1. As can be seen on Figure 6, positive values of s_2 do not give good results, so we can restrict our study to negative values of s_2.

For negative values of s_2, Figure 7 shows that both the ℓ^2 and the ℓ^∞ errors are minimal for a value either equal or close to $s_2^\star = -c$. We have considered different values for s_1 in order to verify that this behaviour does not depend on s_1, no more than it depends on c.

It can be noted that for values of s_2 not too far away from the optimal value $s_2^\star = -c$, the error does not grow much. As a result, the optimal condition is rather not too sharp. Yet going further away from the optimum degrades effectively the error, which denotes that the minimum is significant. We can also notice that the larger the parameter c, the wider the range of values of s_2 which appear quasi-optimal.

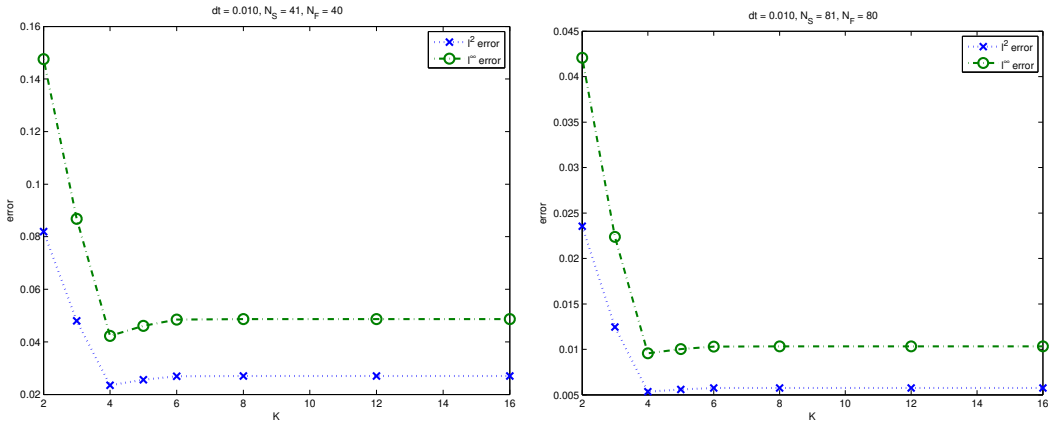

(a) $\delta t = 10^{-2}$, $N_S = 41$, $N_F = 40$ (b) $\delta t = 10^{-2}$, $N_S = 81$, $N_F = 80$

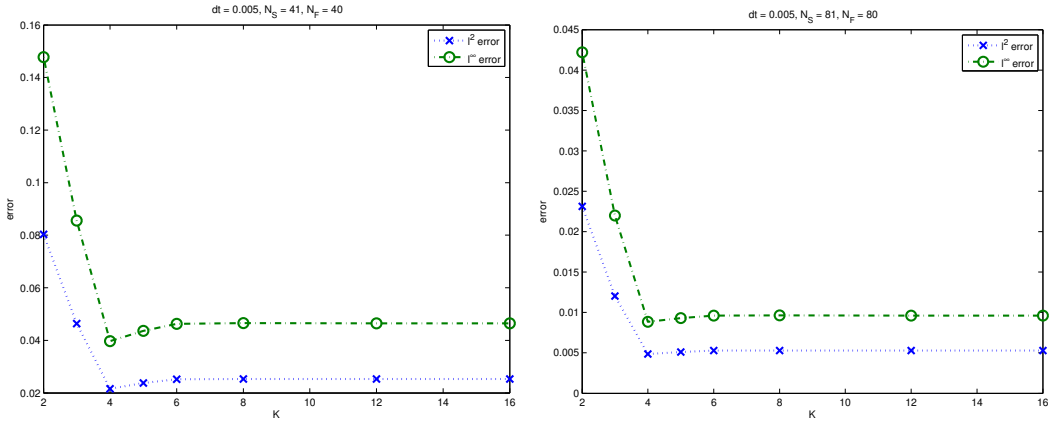

(c) $\delta t = 5 \cdot 10^{-3}$, $N_S = 41$, $N_F = 40$ (d) $\delta t = 5 \cdot 10^{-3}$, $N_S = 81$, $N_F = 80$

Figure 5: ℓ^2 and ℓ^∞ errors with respect to K, for various time and space discretizations.

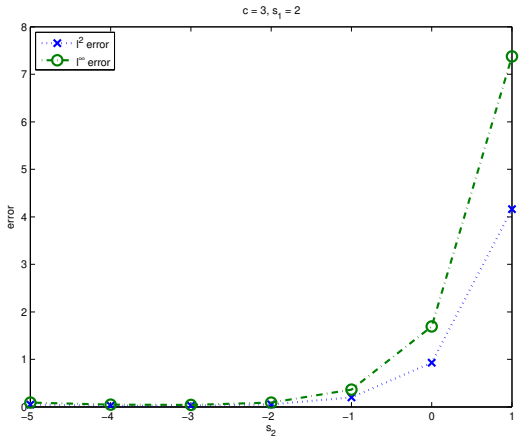

Figure 6: ℓ^2 and ℓ^∞ errors with respect to s_2, for $c = 3$ and $s_1 = 2$. We can see that the error increases steeply for s_2 positive.

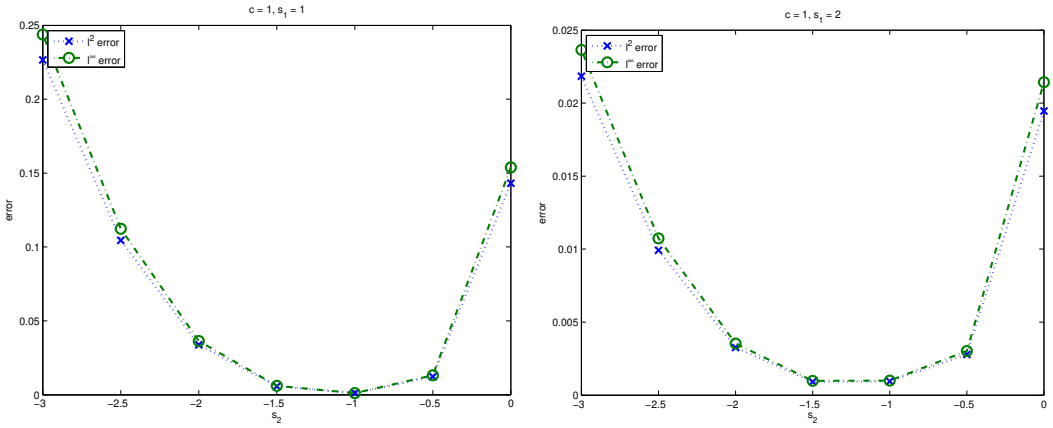

(a) $c = 1$, $s_1 = 1$

(b) $c = 1$, $s_1 = 2$

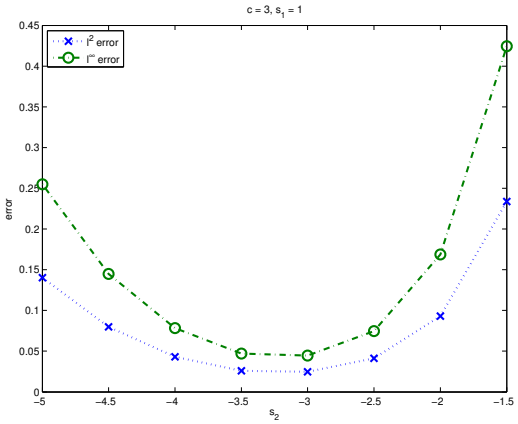

(c) $c = 3$, $s_1 = 1$

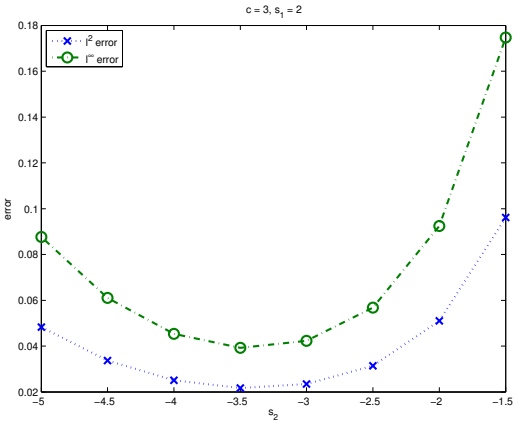

(d) $c = 3$, $s_1 = 2$

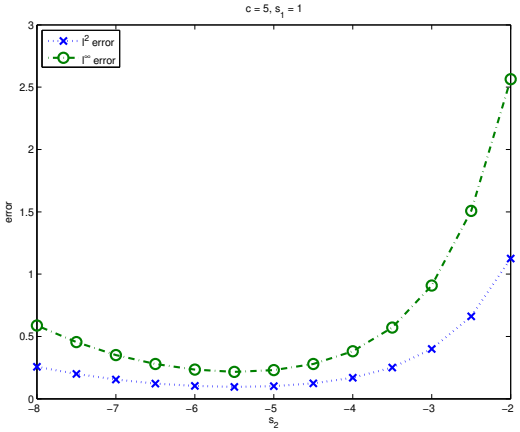

(e) $c = 5$, $s_1 = 1$

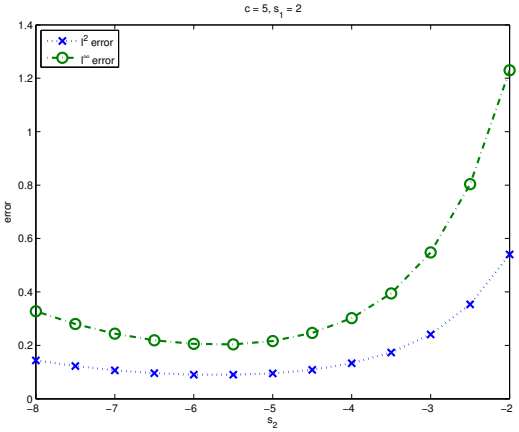

(f) $c = 5$, $s_1 = 2$

Figure 7: ℓ^2 and ℓ^∞ errors with respect to s_2, for $c = 1$ (top), $c = 3$ (middle) or $c = 5$ (bottom), and $s_1 = 1$ (left) or $s_1 = 2$ (right).

4.4 Influence of the parameter s_1

To conclude, we study the effect of the parameter s_1, which is a constant approximation of the symbol of the optimal operator $S_1^\star = \sqrt{\kappa}\,\partial_t^{\frac{1}{2}}$. A first simulation shows that taking s_1 too small does not give good results (Figure 8).

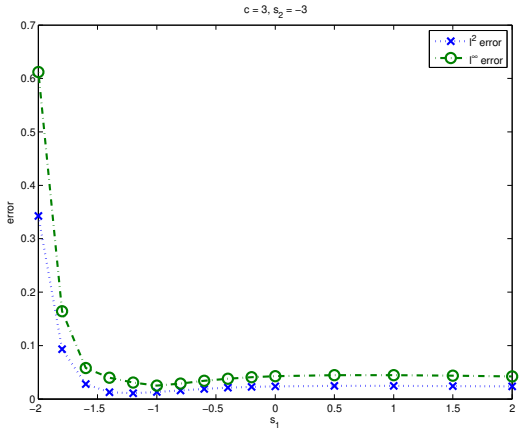

Figure 8: ℓ^2 and ℓ^∞ errors with respect to s_1, for $c = 3$ and $s_2 = -c$. We can see that the error increases sharply for too small s_1.

We then study different situations and take different values of c and of s_2 (optimal and non-optimal values). The profiles we obtain on Figure 9 are not all the same, but in a general way the value of s_1 is of small influence on the error. If small values of s_1 (between 0 and 2) degrade a little the result, there is not an obvious "good choice" of s_1 once s_2 and the other parameters are fixed. Somehow, this can be explained by the fact that we are trying to approximate a symbol of order one-half in the frequency domain, by a constant symbol (of order zero), which can never be very satisfying.

5 Conclusion and perspectives

Much effort has been devoted in the last decade to design efficient algorithms for fluid-structure interaction problems, with emphasis on the reformulation and discretization of interface conditions, using, e.g., Robin-Robin or Robin-Neumann coupling: for instance, see [3, 4, 5, 13, 18, 33] at first, and later on, [8, 9, 10, 16, 21, 22, 23, 24, 45]. Even some first attempts have been made to design parallel-in-time schemes for fluid-structure: see, e.g., [44] for a multiple shooting method, or [12] for an adaptation of the "Parareélle" method.

Present work can be viewed as a very first step in this direction. Indeed, Schwarz-in-time (or Schwarz Waveform Relaxation) methods allow a great flexibility to choose the time-discretization for each subdomain. For instance, different time steps and different solvers can be chosen for each subdomain, according to their relevance: see, e.g., [29]. Since strategies for time-parallel solvers are very different for the parabolic [31, 38] and second-order hyperbolic cases [17, 30], such framework would allow to combine them eventually.

Of course, we considered the simplest setting to start with, and a lot of additional difficulties appear when more complex fluid-structure interaction problems are targeted. For instance, an ongoing work is about the influence of the geometry on the design of optimized conditions, as it has been done in, e.g., [26, 46] in another context. As well, two-dimensional

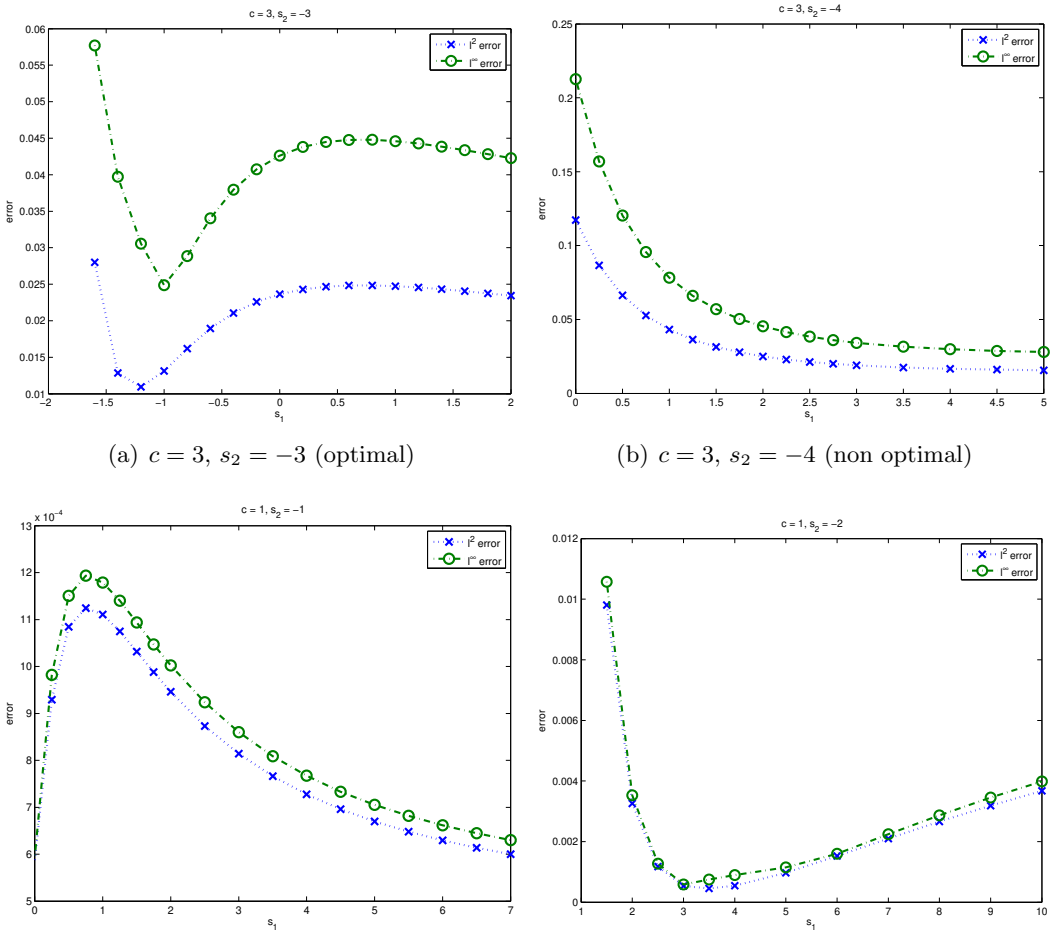

(a) $c = 3$, $s_2 = -3$ (optimal)

(b) $c = 3$, $s_2 = -4$ (non optimal)

(c) $c = 1$, $s_2 = -1$ (optimal)

(d) $c = 1$, $s_2 = -2$ (non optimal)

Figure 9: ℓ^2 and ℓ^∞ errors with respect to s_1, for $c = 3$ (top) and $c = 1$ (bottom), for optimal (left) or non-optimal (right) values of s_2.

and three-dimensional problems should be investigated. Last but not least, for a large class of realistic fluid-structure interaction problems, a very difficult issue is the added-mass effect [11], related to the incompressibility conditions in Stokes or Navier-Stokes equations, that stiffens the coupling between the fluid and the solid when their density are of the same magnitude, and makes the design of efficient partitioned procedures highly challenging [18, 20].

Acknowledgements

The two authors thank Université de Franche-Comté and Région Bourgogne Franche-Comté for funding. They also thank Miguel A. Fernandez, Yvon Maday, Martin Gander, Véronique Martin and Xavier Antoine for stimulating discussions and helpful comments.

References

[1] Robert A. Adams. *Sobolev spaces*. Academic Press, New York-London, 1975. Pure and Applied Mathematics, Vol. 65.

[2] Anton Arnold. Numerically absorbing boundary conditions for quantum evolution equations. *VLSI Design*, 6 (1-4):313–319, 1998.

[3] Matteo Astorino, Franz Chouly, and Miguel A. Fernández. Robin based semi-implicit coupling in fluid-structure interaction: stability analysis and numerics. *SIAM J. Sci. Comput.*, 31(6):4041–4065, 2009/10.

[4] Santiago Badia, Fabio Nobile, and Christian Vergara. Fluid-structure partitioned procedures based on Robin transmission conditions. *J. Comput. Phys.*, 227(14):7027–7051, 2008.

[5] Santiago Badia, Fabio Nobile, and Christian Vergara. Robin-Robin preconditioned Krylov methods for fluid-structure interaction problems. *Comput. Methods Appl. Mech. Engrg.*, 198(33-36):2768–2784, 2009.

[6] Viktor A. Baskakov and Aleksandr V. Popov. Implementation of transparent boundaries for numerical solution of the Schrödinger equation. *Wave Motion*, 14(2):123–128, 1991.

[7] Naoufel Ben Abdallah, Florian Méhats, and Olivier Pinaud. On an open transient Schrödinger-Poisson system. *Math. Models Methods Appl. Sci.*, 15(5):667–688, 2005.

[8] Erik Burman, Rebecca Durst, Miguel A. Fernández, and Johnny Guzmán. Fully discrete loosely coupled Robin-Robin scheme for incompressible fluid-structure interaction: stability and error analysis, 2020. arXiv 2007.03846.

[9] Erik Burman and Miguel A. Fernández. Explicit strategies for incompressible fluid-structure interaction problems: Nitsche type mortaring versus Robin-Robin coupling. *Internat. J. Numer. Methods Engrg.*, 97(10):739–758, 2014.

[10] Shunxiang Cao, Alex Main, and Kevin G. Wang. Robin-Neumann transmission conditions for fluid-structure coupling: embedded boundary implementation and parameter analysis. *Internat. J. Numer. Methods Engrg.*, 115(5):578–603, 2018.

[11] Paola Causin, Jean-Frédéric Gerbeau, and Fabio Nobile. Added-mass effect in the design of partitioned algorithms for fluid-structure problems. *Comput. Methods Appl. Mech. Engrg.*, 194(42-44):4506–4527, 2005.

[12] Franz Chouly and Miguel A. Fernández. An enhanced parareal algorithm for partitioned parabolic-hyperbolic coupling. *AIP Conference Proceedings*, 1168(1):1517–1520, 2009.

[13] Joris Degroote. On the similarity between Dirichlet-Neumann with interface artificial compressibility and Robin-Neumann schemes for the solution of fluid-structure interaction problems. *J. Comput. Phys.*, 230(17):6399–6403, 2011.

[14] Marco Discacciati and Luca Gerardo-Giorda. Optimized Schwarz methods for the Stokes-Darcy coupling. *IMA J. Numer. Anal.*, 38(4):1959–1983, 2018.

[15] Gustav Doetsch. *Anleitung zum praktischen Gebrauch der Laplace-Transformation und der Z-Transformation.* R. Oldenbourg Verlag, Munich, fourth edition, 1981.

[16] M.-P. Errera and F. Duchaine. Comparative study of coupling coefficients in Dirichlet-Robin procedure for fluid-structure aerothermal simulations. *J. Comput. Phys.*, 312:218–234, 2016.

[17] Charbel Farhat, Julien Cortial, Climène Dastillung, and Henri Bavestrello. Time-parallel implicit integrators for the near-real-time prediction of linear structural dynamic responses. *Internat. J. Numer. Methods Engrg.*, 67(5):697–724, 2006.

[18] Miguel A. Fernández. Coupling schemes for incompressible fluid-structure interaction: implicit, semi-implicit and explicit. *SEMA J.*, (55):59–108, 2011.

[19] Miguel A. Fernández, Luca Formaggia, Jean-Frédéric Gerbeau, and Alfio Quarteroni. The derivative of the equations for fluids and structure. In *Cardiovascular mathematics*, volume 1 of *MS&A. Model. Simul. Appl.*, pages 77–121. Springer Italia, Milan, 2009.

[20] Miguel A. Fernández and Jean-Frédéric Gerbeau. Algorithms for fluid-structure interaction problems. In *Cardiovascular mathematics*, volume 1 of *MS&A. Model. Simul. Appl.*, pages 307–346. Springer Italia, Milan, 2009.

[21] Miguel A. Fernández, Mikel Landajuela, Jimmy Mullaert, and Marina Vidrascu. Robin-Neumann schemes for incompressible fluid-structure interaction. In *Domain decomposition methods in science and engineering XXII*, volume 104 of *Lect. Notes Comput. Sci. Eng.*, pages 65–76. Springer, Cham, 2016.

[22] Miguel A. Fernández, Jimmy Mullaert, and Marina Vidrascu. Explicit Robin-Neumann schemes for the coupling of incompressible fluids with thin-walled structures. *Comput. Methods Appl. Mech. Engrg.*, 267:566–593, 2013.

[23] Miguel A. Fernández, Jimmy Mullaert, and Marina Vidrascu. Generalized Robin-Neumann explicit coupling schemes for incompressible fluid-structure interaction: stability analysis and numerics. *Internat. J. Numer. Methods Engrg.*, 101(3):199–229, 2015.

[24] Davide Forti, Alfio Quarteroni, and Simone Deparis. A parallel algorithm for the solution of large-scale nonconforming fluid-structure interaction problems in hemodynamics. *J. Comput. Math.*, 35(3):363–380, 2017.

[25] Martin J. Gander. Optimized Schwarz methods. *SIAM J. Numer. Anal.*, 44(2):699–731, 2006.

[26] Martin J. Gander. On the influence of geometry on optimized Schwarz methods. *SeMA J.*, (53):71–78, 2011.

[27] Martin J. Gander and Laurence Halpern. Méthodes de relaxation d'ondes (SWR) pour l'équation de la chaleur en dimension 1. *C. R. Math. Acad. Sci. Paris*, 336(6):519–524, 2003.

[28] Martin J. Gander, Laurence Halpern, and Frédéric Nataf. Optimal Schwarz waveform relaxation for the one dimensional wave equation. *SIAM J. Numer. Anal.*, 41(5):1643–1681, 2003.

[29] Martin J. Gander, Yao-Lin Jiang, and Rong-Jian Li. Parareal Schwarz waveform relaxation methods. In *Domain decomposition methods in science and engineering XX*, volume 91 of *Lect. Notes Comput. Sci. Eng.*, pages 451–458. Springer, Heidelberg, 2013.

[30] Martin J. Gander and Mădălina Petcu. Analysis of a Krylov subspace enhanced parareal algorithm for linear problems. In *Paris-Sud Working Group on Modelling and Scientific Computing 2007–2008*, volume 25 of *ESAIM Proc.*, pages 114–129. EDP Sci., Les Ulis, 2008.

[31] Martin J. Gander and Stefan G. Vandewalle. Analysis of the parareal time-parallel time-integration method. *SIAM Journal on Scientific Computing*, 29:556–578, 2007.

[32] Martin J. Gander and Tommaso Vanzan. Heterogeneous optimized Schwarz methods for second order elliptic PDEs. *SIAM J. Sci. Comput.*, 41(4):A2329–A2354, 2019.

[33] Luca Gerardo-Giorda, Fabio Nobile, and Christian Vergara. Analysis and optimization of Robin-Robin partitioned procedures in fluid-structure interaction problems. *SIAM J. Numer. Anal.*, 48(6):2091–2116, 2010.

[34] Giacomo Gigante, Giulia Sambataro, and Christian Vergara. Optimized Schwarz Methods for Spherical Interfaces With Application to Fluid-Structure Interaction. *SIAM J. Sci. Comput.*, 42(2):A751–A770, 2020.

[35] Giacomo Gigante and Christian Vergara. Optimized Schwarz method for the fluid-structure interaction with cylindrical interfaces. In *Domain decomposition methods in science and engineering XXII*, volume 104 of *Lect. Notes Comput. Sci. Eng.*, pages 521–529. Springer, Cham, 2016.

[36] Gustaf Gripenberg, Stig-Olof Londen, and Olof J. Staffans. *Volterra integral and functional equations*, volume 34 of *Encyclopedia of Mathematics and its Applications*. Cambridge University Press, Cambridge, 1990.

[37] Houde Han and Zhongyi Huang. A class of artificial boundary conditions for heat equation in unbounded domains. *Comput. Math. Appl.*, 43(6-7):889–900, 2002.

[38] Jacques-Louis Lions, Yvon Maday, and Gabriel Turinici. Résolution d'EDP par un schéma en temps "pararéel". *C. R. Acad. Sci. Paris Sér. I Math.*, 332(7):661–668, 2001.

[39] Jacques-Louis Lions and Enrico Magenes. *Problèmes aux limites non homogènes et applications. Vol. 1.* Travaux et Recherches Mathématiques, No. 17. Dunod, Paris, 1968.

[40] Christian Lubich. Discretized fractional calculus. *SIAM J. Math. Anal.*, 17(3):704–719, 1986.

[41] Yvon Maday. Analysis of coupled models for fluid-structure interaction of internal flows. In *Cardiovascular mathematics*, volume 1 of *MS&A. Model. Simul. Appl.*, pages 279–306. Springer Italia, Milan, 2009.

[42] J.S. Papadakis. Impedance formulation of the bottom boundary condition for the parabolic equation model in underwater acoustics. *NORDA Parabolic Equation Workshop, NORDA Tech. Note*, 143, 01 1982.

[43] Igor Podlubny. *Fractional differential equations*, volume 198 of *Mathematics in Science and Engineering*. Academic Press, Inc., San Diego, CA, 1999.

[44] Thomas Richter and Thomas Wick. On time discretizations of fluid-structure interactions. In *Multiple shooting and time domain decomposition methods*, volume 9 of *Contrib. Math. Comput. Sci.*, pages 377–400. Springer, Cham, 2015.

[45] Anyastassia Seboldt and Martina Bukač. A non-iterative domain decomposition method for the interaction between a fluid and a thick structure, 2020. arXiv 2007.00781.

[46] Yingxiang Xu. The influence of domain truncation on the performance of optimized Schwarz methods. *Electron. Trans. Numer. Anal.*, 49:182–209, 2018.

[47] Xu Zhang and Enrique Zuazua. Long-time behavior of a coupled heat-wave system arising in fluid-structure interaction. *Arch. Ration. Mech. Anal.*, 184(1):49–120, 2007.

[48] Chunxiong Zheng. Approximation, stability and fast evaluation of exact artificial boundary condition for the one-dimensional heat equation. *J. Comput. Math.*, 25(6):730–745, 2007.